Exploring the Dynamic Heterogeneity at the Interface of a Protein in Aqueous Ionic Liquid Solutions

Krishna Prasad Ghanta, Sandip Mondal, and Sanjoy Bandyopadhyay*

Molecular Modeling Laboratory, Department of Chemistry, Indian Institute of Technology, Kharagpur - 721302, India

E-mail: sanjoy@chem.iitkgp.ac.in

Abstract

Room temperature molecular dynamics (MD) simulations of the globular protein α-lactalbumin in aqueous solutions containing BMIM (1-butyl-3-methylimidazolium) based ionic liquids (ILs) with a series of Hofmeister anions have been carried out. In particular, effects of anions of different shapes/sizes and hydrophobic/hydrophilic characters, namely, thiocyanate (SCN^-), dicyanamide (DCA^-), methyl sulphate (MS^-), triflate (TFO^-) and bis(trifluoromethane) sulfonimide (TF_2N^-) on the heterogeneous dynamic environment at the interface around the protein have been explored. The calculations revealed exchange of population between water and IL cation-anion components beyond the first layer of bound water molecules at the protein surface. Further, increasingly restricted diffusivity of the IL components and water around the protein have been found to be associated with longer time scale for the onset of dynamic heterogeneity at the interface. Restricted diffusivity of water molecules at the interface in presence of the ILs have been found to be correlated with longer time scale of structural relaxations of protein-water (PW) hydrogen bonds at the interface. More importantly, the time scale associated with the reorientations of the anions have been found to be anticorrelated with their translational diffusivity, the effect being more at the interface as compared to the bulk IL solutions. It is demonstrated that nonuniform ability of the anions to form hydrogen bonds with water due to their differential shapes and hydrophilic characters is the origin behind such anticorrelation.

1 INTRODUCTION

α-Lactalbumin is an important calcium containing milk protein consisting of 123 amino acid residues in its structural unit. The tertiary structure of the protein contains three major α-helices and an antiparallel β-sheet comprising of two β-strands along with two 3_{10} helices and several turns and coils inerconnecting the secondary structural units. It catalyses galactosyl transferase by converting the galactosyl residue of UDP-galactose to N-acetylglucosamine to form lactose in human body.[1] It is known that the sparseness of α-lactalbumin triggers the growth of breast cancer.[2] Among different methods of treatment, vaccination by α-lactalbumin has a major advantage as it can specifically target and destroy the cancer cells.[3]

Room temperature ionic liquids, henceforth denoted as ILs, form an important class of molten organic salts with cation-anion pairs comprising of organic cations and organic/inorganic anions. ILs in their molten states exhibit fascinating physico-chemical characteristics, such as low vapor pressure, high thermal stability and viscosity, non-volatility and non-toxicity.[4,5] ILs are known to act as bio-catalysts and have the ability to perpetuate the structural stability and activity of bio-molecules.[6,7] Due to low vapor pressures, ILs are often used as "green" solvents in bio-molecular reactions.[8,9] Importantly, the physico-chemical properties of ILs can be suitably tuned by varying the cation-anion conbinations, thereby often making those more efficient than regular organic solvents.[10]

Structural stabilities of proteins and their functions are known to be sensitive to the presence of ILs in aqueous medium.[6,7,11] Thus, to obtain a generic understanding of the action of ILs on proteins, it is important to elucidate the protein-IL interactions and probe the modified dynamic environment at the protein interface in aqueous solutions containing ILs with distinctly different cation-anion combinations. Significant efforts have been made in recent times to study protein-IL interactions and their consequence on structural stability and functions of proteins.[12–14] Despite such efforts, conflicting reports on the influence of

ILs on proteins exist in the literature.[15–18] On one hand, there are evidences that suggest that ILs can play key roles in protein refolding,[15,16] while on the other, ILs are also found to destabilize protein structures as denaturants.[17,18] In a recent study, Liem *et al*[19] examined the impact of pyrrolidinium and imidazolium based ILs on green fluorescent protein (GFP) using UV-Vis and NMR spectroscopic techniques. They demonstrated that the choice of the anion component of an IL plays a vital role in determining protein-IL interactions and hence the structural stability of the protein. Earlier, Cabrita and co-workers[17] elucidated the effect of imidazolium-based ILs on protein stability based on experimental and MD simulation studies. It was demonstrated that the preferential binding of the IL anions with the positively charged protein residues leads to partial dehydration of the protein backbone. Isothermal titration calorimetry (ITC) and circular dichroism (CD) techniques have been used recently to probe the thermal stability of bovine serum albumin (BSA) in presence of surface-active ILs.[20] It is found that the stabilization of BSA occurs in presence of fluorinated ILs (FILs). Effects of imidazolium and guanidium based ILs on the stability of lipase enzyme (CAL-B) have been studied using MD simulations.[21] Based on the calculations, the stability of CAL-B in ILs containing different anions follows the order $NO_3^- << BF_4^- < PF_6^-$. Attempts have also been made to establish the correlation between the stability of a protein and the distribution of IL components at the interface.[22] In a series of studies, interesting structural and dynamical properties of imidazolium based ILs within the solvation shells of ubiquitin and zinc finger motif (ZNF) have been reported by Haberler *et al*.[23,24] It is observed that the IL cations accumulate at the surface of ZNF due to formation of strong anion-water network. On the other hand, two states of transformation of the solvation shell around ubiquitin have been noticed in aqueous IL solutions. It is found that the pure aqueous system first transforms into an ionic solution followed by further changes to ionic liquid melt.

Hofmeister series anions based on their influence on water structure around proteins have been classified into two types, namely, kosmotropes and chaotropes.[25,26] Kosmotropes

are anions with high charge densities capable of forming strong hydrogen bonding network with water, and thus can stabilize protein structure. In contrast, chaotropic anions with low charge densities tend to form direct protein-anion hydrogen bonds by breaking protein-water hydrogen bonds, thereby destabilizing the protein structure. The Hofmeister anions in terms of their effects on protein stability have been arranged as, $O_4{}^{-2} > dhp^- > Ac^- > F^- > Cl^- > || Br^- > I^- > SCN^-$, where || denotes the crossover point between stabilizing and destabilizing influence of the anion series.[27] Importantly, it is reported that the predicted effect on protein stability by different ions may often deviate from the above order.[28,29] Such apparent anomalous effect of Hofmeister anions on protein stability has been attributed to specific complex structures of proteins and their interfacial geometry.[30]

It is known that the local structural and dynamical complexities within the solvation layer in close proximity to a protein play defining roles in controlling the protein conformation, its structural stability and biological activity.[8,31] Addition of ILs containing different types of Hofmeister anions as co-solvents in aqueous medium are expected to significantly alter the dynamic environment at the surface of the protein. However, despite the importance of the problem, microscopic understanding of the effects of IL anions on the time scale associated with different dynamic processes at the interface of a protein is still not clear. Efforts have been made in the present work to obtain a generic understanding of how aqueous solutions containing BMIM-based ILs with different Hofmeister anions influence the dynamic heterogeneity at the interface of the globular protein α-lactalbumin. In particular, effects of anions of different shapes/sizes and hydrophobic/hydrophilic characters on the time scales associated with the translational and reorientational motions of different components at the interface and their correlation with the dynamics of hydrogen bonds have been explored in detail. The rest of the article has been organized as follows. We have documented in brief the protocols followed to set up different simulation systems and the methdologies employed in Section 2. Elaborate description of the results as obtained from the analyses is provided

in Section 3. Finally, in Section 4 we have highlighted the important findings from our study and the conclusions reached based on that.

2 COMPUTATIONAL DETAILS AND METHODOLOGY

MD simulations of the globular protein α-lactalbumin have been carried out at room temperature (298 K) in aqueous solutions containing 2M concentration of BMIM-based ILs with five different Hofmeister anions, namely, SCN^-, DCA^-, MS^-, TFO^- and TF_2N^-. GROMACS-2018 MD simulation tool has been used to carry out all the calculations.[32] The initial coordinates of the protein was adopted from high resolution x-ray diffraction data[33] with Protein Data Bank (PDB) ID: 1HFX. We have employed OPLS-AA force field for the protein[34] and the IL components (cations and anions),[35] while the mTIP3P model[36] (modified version of TIP3P) was used for water. The N- and C-terminal residues of the protein were protected by capping those with acetyl and N-methyl groups, respectively. The initial configurations of different simulation systems were prepared by using the PACKMOL package.[37] An orthorhombic cell (65Å$\times$ 67Å$\times$ 75Å) with the protein molecule being placed at the center was used to prepare each of the systems. The IL components were then ramdomly inserted within the cell with a minimum separation of 10 Å from the protein surface. To balance the excess negative charge of the protein, seven Na^+ ions were added in each case. The numbers of IL cations/anions and water molecules corresponding to 2M concentration of the solution for different systems are listed in Table 1. LINCS algorithm[38] was used to constrain the covalent bonds involving hydrogen atoms for the protein, IL and water molecules.

Steepest descent energy minimization method as implemented in GROMACS package[32] was first used for 10,000 steps to remove the initial stress and unfavorable contacts for each system. Following this, the systems were heated from 0 K to a high temperature of 450 K

with a progressive heating rate of 30 K per 100 picoseconds (ps), and then quenched down to 298K at the same rate. This process was carried out using the Berendsen barostat and velocity rescale thermostat method with a stochastic term.[39,40] Positional restraints on the protein non-hydrogen atoms were applied during the heating and cooling cycles to avoid any unphysical conformational change of the protein due to change in temperature. Each simulation system was then equilibrated for 10 nanoseconds (ns) duration following removal of positional restraints on the protein under isothermal-isobaric (NPT) ensemble conditions at 298 K and 1 bar pressure. The pressure was controlled by the Berendsen barostat method,[39] and temperature controlling was done by employing the velocity rescale thermostat approach with a stochastic term.[40] At this point, the simulation conditions were changed from NPT ensemble to that of NVT (isothermal-isochoric) ensemble using the velocity rescale thermostat approach with a stochastic term,[40] and the equilibration stage was continued for another 10 ns duration. This was then followed by 500 ns long NVT production run for each system using the Nose-Hoover thermostat approach.[41] We have employed 2 femtosecond (fs) integration time step, and the trajectories were saved with 400 fs time resolution for the analyses. The short-range Lennard-Jones interactions were computed with a spherical cut-off distance of 12 Å, and the long-range electrostatic interactions were computed by using the particle-mesh Ewald summation method.[42] For comparative analyses, we have carried out another set of five simulations with 2M aqueous IL solutions with the same set of five different anions in absence of the protein molecule. 100 ns trajectory was generated for each of the five systems following the same protocols as discussed above. Note that the results presented on the microscopic properties of the IL components and water in presence of the protein are calculated by splitting the final 220 ns trajectory for each case into 20 blocks, each block of 10 ns duration with a separation of 1 ns between two successive blocks. Similarly, the final 55 ns trajectory for each of the IL-water systems in absence of the protein molecule was splitted into 5 such blocks to compute the corresponding properties.

3 RESULTS AND DISCUSSION

In an earlier report,[43] we studied in detail the effects of aqueous IL solutions containing $BMIM^+$ cations with different anions of varying degree of hydrophobic/hydrophilic character on the conformational properties of the globular protein α-lactalbumin. The calculations revealed contrasting effects of the ILs with different hydrophilicity on protein conformation. Compared to hydrophilic ILs, the protein structure was found to become more rigid with reduced conformational fluctuations in presence of hydrophobic ILs. In particular, depletion of water at the protein surface due to stronger protein-IL interaction in presence of hydrophilic ILs has been identified as the origin behind increased flexibility and reduced stability of the protein in aqueous solution containing hydrophilic ILs. In the present study, we make attempts to explore how the nonuniform distribution of ILs of different types modifies the dynamically heterogeneous environment at the interface of a protein in aqueous IL solutions. In particular, the distributions of different components of aqueous BMIM-based IL solutions containing different Hofmeister series anions (SCN^-, DCA^-, MS^-, TFO^- and TF_2N^-) and their microscopic dynamical characteristics at the interface of the globular protein α-lactalbumin have been characterized in detail.

3.1 Distributions of IL and Water Components at the Interface

In this section we investigate how the IL components comprising of $BMIM^+$ cations and different Hofmeister anions (A^-) and water molecules in aqueous IL solutions are distributed at the surface of the protein. For that, we have calculated the number density profiles ($\rho(r)$) of the IL components and water molecules as a function of distance from the protein surface for different systems. The calculation has been carried out by considering the actual volume accessible to the IL and water components within a spherical shell of radius r and thickness δr around the protein, instead of the entire volume of the spherical shell. This provides a

more accurate measure of $\rho(r)$ around the non-spherical heterogeneous surface of a protein as compared to that obtained from regular spherical volume consideration. We have employed a Monte Carlo random mumber insertion method[44] to compute the accessible volume around the protein. The density profiles ($\rho(r)$) are then obtained by dividing the numbers of different components by the corresponding accessible volumes. The results obtained are displayed in Figure 1. The figure represents interesting local density distributions of water (solvent) and IL (co-solvent) components near the protein surface. Expectedly, we notice depletion of water density at the interface in presence of IL (Figure 1(c)). However, it can be seen that inspite of reduced water density, the protein is almost exclusively surrounded by a first layer of water molecules (within around 3–4 Å) that are bound to its residues. The data reveal exchange of population between water and the IL cations and anions around the protein beyond the first shell of bound water molecules, resulting in increased density of IL components at the interface (within around 4–6 Å) as compared to that in the bulk water-IL solution away from the protein surface. We have listed the average numbers of $BMIM^+$ cations (N_{BMIM^+}) and different anions (N_{A^-}) along with that of the water molecules (N_W) present within 6 Å from the protein surface as obtained from the simulated trajectories in Table S1 of the Supporting Information. It can be seen that compared to the protein in pure water, presence of the ILs around the protein in aqueous IL solutions leads to 30–40 % reduction in number of water molecules at the interface. Interestingly, Figure 1 reveals significantly heterogeneous local density distributions of the IL components at the interface for different systems, which is often extended over longer distance (9–10 Å) from the protein.

Nonuniform distributions of the IL cations and anions around the protein with expulsion of a fraction of water molecules from the interface are likely to be correlated with the interaction strengths between the protein and the IL ion pairs (E_{P-IL}) and that between the protein and water (E_{P-W}). We have calculated the average interaction strengths ($\langle \mathrm{E_{P-IL}} \rangle$ and $\langle \mathrm{E_{P-W}} \rangle$) for the IL components and the water molecules that are present around the protein

(within 6 Å) in different systems. It is found that the $\langle E_{P-IL} \rangle$ values for different systems vary within –35 to –40 kcal mol^{-1} as compared to the corresponding $\langle E_{P-W} \rangle$ values varying within –22 to –25 kcal mol^{-1}. Thus, it is clear that relatively stronger interaction strengths between the protein and IL ion pairs as compared to that between the protein and water results in expulsion of a fraction of water molecules from the interface with simultaneous accumulation of IL components. It may be noted that the $BMIM^+$ cation being common, its density distribution is nearly homogeneous in all systems, except for the aqueous solution containing [BMIM][TF_2N] as the IL. On the other hand, compared to the $BMIM^+$ cations, density distributions of different anions (A^-) around the protein surface have been found to be highly nonuniform (Figure 1(b)). It can be seen that MS^- and TFO^- anions exhibit noticeably higher density near the protein (within ∼6 Å) as compared to the other anions (SCN^-, DCA^- and TF_2N^-). It is apparent that different shapes/sizes of the anions employed play an important role in guiding the orientation and packing of the anions at the interface and hence the density profiles. The result shows that MS^- and TFO^- anions being spherical in shape can pack around the protein in a more efficient manner, thereby leading to their higher densities at the interface. In comparison, SCN^- is linear in shape while DCA^- is angular. Due to such non-spherical geometries, SCN^- and DCA^- anions cannot orient and pack around the protein as effectively as the spherical ones (MS^- and TFO^-). Further, presence of two large flexible sub-units around the central nitrogen atom of TF_2N^- prevents it from approaching the protein surface as evident from the data. Non-preferential packing of SCN^-, DCA^- and TF_2N^- anions around the protein due to different sizes and non-spherical shapes leads to their reduced local densities at the interface, which are nearly similar to that observed away from the protein into the bulk. It is further apparent that non-preferential distribution of TF_2N^- anions at the interface also prevents the cationic counterparts ($BMIM^+$) to approach near the protein, as evident from Figure 1(a).

3.2 Dynamical Properties at the Interface

It is revealed from our discussion above that the presence of BMIM-based ILs containing different Hofmeister series anions (A^-) of varying shapes/sizes results in nonuniform distributions of the IL components at the interface of the globular protein α-lactalbumin. Such nonuniform cation-anion distributions along with expulsion of a fraction of water molecules from the interface are expected to modify the dynamic environment around the protein in a heterogeneous manner. Attempts have been made in the following sections to explore in detail such dynamic heterogeneity at the interface in different aqueous IL solutions. It may be noted that the calculations are averaged over the water molecules and the IL cations and anions that at a given instant of time are found to be within 6 Å from the protein surface. This broadly represents the solvation shell around the protein, as the water (solvent) and IL components (co-solvent) present in it are involved in strongly interacting with the protein.

3.2.1 Translational Motions at the Interface

Translational motions of the IL components (cations and anions) and water molecules around the α-lactalbumin protein (within 6 Å) in different aqueous IL solutions have been investigated by measuring their mean square displacements (MSD) as a function of time. MSD ($\langle \Delta r^2 \rangle$) is defined as[45]

$$\langle \Delta r^2 \rangle = \langle |r_i(t) - r_i(0)|^2 \rangle \tag{1}$$

where $r_i(t)$ and $r_i(0)$ correspond to the position vectors of the center-of-mass of the i-th tagged component around the protein at time t and at $t = 0$, respectively. The angular brackets signify that the averaging is carried out at different time origins. The results as obtained from our calculations are depicted in Figure 2. As a reference, the corresponding result for water present at the interface of the protein in pure aqueous medium in absence of any IL is included in Figure 2(c). This is done by performing an MD simulation of the

protein in water in absence of any IL following the same protocols as described In Section 2. MSDs of the cation-anion components and water molecules in different bulk aqueous IL solutions in absence of the protein have also been computed and presented in Figure S1 of the Supporting Information for comparison. The data for pure bulk water as obtained from an MD simulation of mTIP3P water under same conditions is included in Figure S1(c). The estimated errors involved in the calculations as obtained from the standard deviations of the data presented are found to be small (within 5%). To quantify further, we have calculated the diffusion coefficients (D_E) of the IL ions and water present at the interface from the slopes of the corresponding MSD data using Einstein's relation[45]

$$D_E = \lim_{\Delta t \to \infty} \frac{\langle \Delta r^2 \rangle}{2d\Delta t} \tag{2}$$

where d is the dimensionality of the system, assumed to be three for the present study. The calculated D_E values are shown in the insets of Figure 2. Similar data for different constituents in aqueous IL solutions in absence of the protein are presented in the insets of Figure S1. Compared to water in pure bulk state, restricted translational mobility of water in presence of IL as co-solvent as evident from Figure S1 signifies increased viscosity of aqueous IL solutions. It is known that the viscosity of an aqueous IL solution depends on the relative hydrophobic/hydrophilic character of the IL components.[46] Our calculation shows that increased size and hydrophobic character of the anions leads to their significantly restricted diffusion. Additionally, though the cations are same ($BMIM^+$) in all systems, but they exhibit nonuniform diffusion time scale which is strongly correlated with that of the corresponding anion counterparts (A^-) (Figure S1(a)). Restricted dynamics of water around a protein in pure aqueous medium is known,[47,48] which is evident from our result too (see Figures 2 and S1). However, more importantly, the data presented in Figure 2 reveal that in addition to increasingly restricted water mobility at the interface, the presence of the protein

in aqueous IL solutions also leads to further restricted dynamics of the IL ion pairs around it. The effect has been found to be nonuniform for different ILs. Consistent with binary water-IL solutions, the degree of restriction increases with increased hydrophobic character of the IL anion. For example, TF_2N^- being most hydrophobic among different anions used, the cation-anion components of the IL [BMIM][TF_2N] exhibit most sluggish correlated dynamics around the protein as compared to the hydrophilic ILs (say, [BMIM][SCN] and [BMIM][DCA]). Another important point to be noted is the existence of three distinct time scales associated with the correlated cation-anion translational motions of different ILs in pure aqueous solutions, as evident from the D_E values (see Figure S1). SCN^- and DCA^- being hydrophilic and non-spherical with relatively smaller size exhibit much faster motions along with their $BMIM^+$ cation counterparts, while TF_2N^- being heavier and hydrophobic, ion pairs in [BMIM][TF_2N] IL solution exhibit drastically slower mobility. On the other hand, due to intermediate hydrophobic character of the anions, ion pairs in [BMIM][MS] and [BMIM][TFO] exhibit diffusion at an intermediate time scale. Presence of the protein largely maintain such difference in diffusion time scale of the cation-anion components of different ILs at the interface, as evident from Figure 2. Interestingly, careful examination of the result reveals a reverse trend in translational motions of water in presence of different ILs. It is apparent that water molecules in presence of a slower hydrophobic IL (e.g., [BMIM][TF_2N]) exhibit relatively faster dynamics as compared to water in presence of a faster hydrophilic IL (e.g., [BMIM][SCN]). Such reverse trend in water dynamics also exists at the interface of the protein (Figure 2) with an increasingly restricted time scale. It signifies that due to strong hydrophobic nature of TF_2N^-, the cation-anion pairs of [BMIM][TF_2N] are not effectively hydrated, thereby leading to relatively faster dynamics of water in pure IL-water solution as well as near the surface of the protein. On the other hand, SCN^- being smaller and hydrophilic in nature are more effectively hydrated. As a result, water molecules in aqueous solution containing [BMIM][SCN] exhibit more restricted diffusivity, the effect increases

further near the surface of the protein.

3.2.2 Residence Times of IL and Water at the Interface

It is apparent from the above discussion that BMIM-based ILs containing Hofmeister anions of different shapes/sizes and hydrophobic/hydrophilic characters exhibit heterogeneously restricted diffusivity near the surface of the protein α-lactalbumin. Such dynamical behavior of the IL components have been found to be anticorrelated with that of the interfacial water molecules. We now probe how the nonuniform dynamical environment around the protein in aqueous IL solutions influences the residence times of the IL ion pairs and water molecules at the interface. For that, we have calculated the residence time correlation function (TCF), $S_R(t)$, for the cation and anion components of the ILs and the water molecules within 6 Å from the protein surface. $S_R(t)$ is defined as[49]

$$S_R(t) = \frac{\langle b(0)B(t)\rangle}{\langle b(0)b(0)\rangle} \tag{3}$$

where, $b(0)$ and $B(t)$ are two population variables that can take two values, either zero or unity. The value of $b(0)$ is unity when a particular type of ions or water molecules are found within the cut-off distance around the protein (6 Å) at time $t = 0$, and zero otherwise. On the other hand, the value of $B(t)$ is unity when a particular component (ion or water) is present within the protein solvation shell (6 Å) continuously from time $t = 0$ to a later time t, and zero otherwise. The angular brackets denote that the results are obtained by averaging over different reference time origins. According to the definition, $S_R(t)$ corresponds to the probability that a particular component (IL ion pair or water) remains continuously within the solvation shell around the protein as defined starting from $t = 0$ to a later time t. Thus, relaxation of $S_R(t)$ provides a true estimate of the residence time of a component at the interface.

The relaxations of $S_R(t)$ for the IL ion pairs and water molecules around the protein for different systems are displayed in Figure 3. The errors involved in the calculation are found to be small (within 2–3%). Heterogeneous relaxation patterns of $S_R(t)$ for different components as evident from the figure are found to be correlated with their translational mobility at the interface, as discussed earlier (Figure 2). Slower dynamics of the IL ion pairs is associated with slower relaxation of $S_R(t)$, indicating longer residence times at the interface and vice versa. The effect is maximum for the most hydrophobic IL ([BMIM][TF_2N]) and minimum for the hydrophilic ones ([BMIM][SCN] and [BMIM][DCA]), as evident from Figure 3. To obtain a quantitative estimate of the residence times of the IL components at the protein surface for different systems, we have fitted the $S_R(t)$ relaxation curves with multi-exponentials of the form

$$S_R(t) = \sum_{i=1}^{N} A_i \exp(-t/\tau_i) \tag{4}$$

where N represents the minimum number of terms required for best fits, while τ_i and A_i represent the characteristic time constants and amplitudes, respectively. We have found that the data presented in Figure 3 are best fitted with $N = 4$. The amplitude-weighted average residence times, $\langle \tau_R \rangle$, as obtained from the data are presented in Table 2. It can be seen that the hydrophobic TF_2N^- anions with significantly restricted diffusivity reside at the interface over 4–10 times longer duration as compared to the fast moving hydrophilic SCN^- and DCA^- anions. Note that due to correlated motions between the cation-anion pairs as discussed earlier, the average residence time of $BMIM^+$ cations in presence of TF_2N^- anions is 2–3 times longer than that in presence of SCN^- and DCA^- anions. Interfacial water molecules being more dynamic than the IL ion pairs exhibit relaxation of $S_R(t)$ on a much faster time scale as evident from Figure 3(c). As a result, the average residence times of water molecules at the interface have been found to be much shorter (often by an order of magnitude or more) as compared to the IL components (see Table 2). Interestingly, we find

that the presence of ILs containing Hofmeister anions of different degrees of hydrophobicity influences the relaxation of $S_R(t)$ and hence the $\langle\tau_R\rangle$ of the interfacial water molecules in a differential manner, though the effect being less as compared to the IL ion pairs. Consistent with water diffusivity near the protein surface in presence of different ILs, it is apparent that more dynamic water molecules at the interface in presence of hydrophobic IL [BMIM][TF_2N] exhibit noticeably shorter residence time as compared to water in presence of other relatively more hydrophilic ILs.

3.3 Dynamic Heterogeneity at the Interface

ILs present in pure state or in aqueous solutions are known to exhibit dynamic heterogeneity (DH),[50–53] a phenomenon that arises in both spatial and temporal domains, and is characterized by deviations in properties from that of purely homogeneous solutions. In the present study, we have demonstrated that the BMIM-based ILs with a number of Hofmeister anions of different shapes/sizes, and varying degrees of hydrophobic/hydrophilic characters exhibit nonuniform diffusivity that is anticorrelated with that of water at the interface of the protein α-lactalbumin. It would be interesting to examine how the presence of the protein in aqueous IL solutions influences the onset of microscopic DH and the corresponding time scale for different components (IL ion pairs and water) within the solvation environment around the protein. We explore that in this section by calculating the non-Gaussian dynamical heterogeneity parameter (DHP), $\alpha_2(t)$,[54,55] and the self-part of the van Hove correlation function, $G_s(r,t)$,[56] for the IL cations and anions, and water molecules present in close proximity to the protein (within 6 Å) in different systems. The non-Gaussian DHP is defined as

$$\alpha_2(t) = \frac{3\langle|\Delta r^4(t)|\rangle}{5\langle|\Delta r^2(t)|\rangle^2} - 1 \tag{5}$$

where, $|\Delta r(t)|$ is the displacement of the tagged particle (IL component or water) at time t. $\alpha_2(t)$ provides the extent of deviation in the distribution of the displacement r of a species from Gaussian distribution at time t. For a dynamically heterogeneous system, starting from the value zero at $t = 0$, the DHP attains a maximum value at some intermediate time before becoming zero again at $t \to \infty$. On the other hand, the self part of van-Hove correlation function is defined as,

$$G_s(r,t) = \frac{1}{N}\langle \sum_{i=1}^{N} \delta(r + r_i(0) - r_i(t)) \rangle \tag{6}$$

where, $r_i(0)$ and $r_i(t)$ corresponds to the positions of the i-th tagged particle at time t=0 and at t, respectively. N represents the number of different components (ions or water molecules) present in the system. G_s(r,t) quantifies the probability of the i-th molecule diffusing from its initial position $r_i(0)$ to the position $r_i(t)$ at time t. The function shows Gaussian behavior for an homogeneous system.[57,58] However, for an heterogeneous mixture, the $\alpha_2(t)$ value is expected to deviate from zero and the corresponding function $G_s(r,t)$ becomes non-Gaussian in nature.[59]

The time evolution of the DHP ($\alpha_2(t)$) for different components (IL cations-anions and water molecules) present in close proximity to the protein (within 6 Å) are depicted in Figure 4. The corresponding data for bulk aqueous IL solutions in absence of the protein are shown in the insets of the figure. The average times associated with the attainment of maximum dynamic heterogeneity ($\langle \tau_D \rangle$) for different components at the interface along with that for bulk aqueous IL solutions as obtained from the figure are listed in Table 3. The errors associated with the calculation have been found to be within 3%. A systematic development of DH with time at the interface is evident from the figure. Compared to pure aqueous IL solutions, greater $\alpha_2(t)$ peak heights for different components around the protein signifies increasing extent of DH at the interface. However, more importantly, the data reveal that the time scale associated with the onset of maximum DH for different components at the

interface within the solvation layer of the protein is significantly longer and nonuniform as compared to that observed in aqueous IL solutions in absence of the protein. It is apparent from Table 3 that the $\langle \tau_D \rangle$ values for water around the protein in presence of different ILs are more than two orders of magnitude longer as compared to that for water in pure aqueous IL solutions. We further notice that the presence of the protein also leads to significantly longer $\langle \tau_D \rangle$ values for the IL components at the interface as compared to pure aqueous IL solutions. The present result shows that such longer time scale for the onset of DH at the interface is correlated with increasingly restricted diffusivity of the IL components and water around the protein as discussed earlier (Figure 2). It is apparent that in most cases, slower diffusivity at the interface leads to longer duration ($\langle \tau_D \rangle$) to attain DH and vice versa. This is particularly evident for the IL ion pairs containing hydrophobic TF_2N^- anions, which exhibit slowest diffusivity at the interface and hence require maximum duration to attain DH, as compared to the other ILs containing either hydrophilic anions or anions with reduced degree of hydrophobicity. It may be noted that due to heterogeneous nature of the protein surface and nonuniform interaction contributions, the effect on $\langle \tau_D \rangle$ values of ILs containing anions of varying degree of hydrophobic/hydrophilic character can be nonuniform, as evident from Table 3.

To further quantify the space-time correlation among different components at the interface around the protein, we have calculated the self-part of the van Hove correlation function $G_s(r,t)$ (see eq. 6) for the cation/anion components of the ILs and water molecules which were initially present near the protein surface. In particular, we have calculated the probability distributions associated with the $BMIM^+$ cations and different anions (A^-) along with that of water molecules which were present at the interface (within 6 Å from the protein) at time t=0 to have moved a particular distance r at different time intervals (100, 500 and 1000 ps for the IL ion pairs, and 20, 50 and 100 ps for water). A relatively shorter time interval is considered for water due to its faster diffusivity as compared to the ions. The

results as obtained for different systems are presented in Figure 5. The data for pure binary aqueous IL solutions are shown in the insets of the figure for comparison. Once again, the errors involved in the calculations are found to be rather small, varying within 2-3 %. Non-Gaussian nature of the distributions for the IL cation/anion components even at longer times is evident from the figure. Similar behavior has also been noticed for water molecules, though the time scale involved is relatively shorter as compared to the cation-anion pairs. The effect is more evident near the protein surface as compared to pure aqueous IL solutions. Such time evolution of $G_s(r,t)$ at the interface is consistent with increasingly restricted mobility and longer residence times of the IL components and water within the solvation layer around the protein, and correlates well with longer time scale required for the onset of maximum DH at the interface, as discussed before. Furthermore, existence of three distinctly different diffusion time scales of the IL components comprising of anions of different degrees of hydrophobic/hydrophilic character as discussed earlier (see Figure 2) is evident from the distribution pattern of $G_s(r,t)$. Due to strong interactions between the protein and the IL components (see Section 3.1), the effect is more significant and prevalent over noticeably longer duration at the interface as compared to bulk aqueous IL solutions, as evident from Figure 5.

3.4 Reorientational Motion at the Interface

So far, we have discussed how the heterogeneous translational motions of the IL components comprising of $BMIM^+$ cations and a series of Hofmeister anions (A^-) with widely different shapes/sizes and hydrophobic/hydrophilic characters are modified near the surface of the protein α-lactalbumin, and their correlation with the time scale of dynamic heterogeneity at the interface. In this section, we investigate how the reorientational motions of the IL cation-anion pairs and water molecules are modified around the protein. This is done by

calculating the reorientational time correlation function (TCF), $C_1(t)$, defined as[60]

$$C_1(t) = \frac{\langle P_1[\hat{u}_i(t) \cdot \hat{u}_i(0)]\rangle}{\langle P_1[\hat{u}_i(0) \cdot \hat{u}_i(0)]\rangle} \tag{7}$$

where, P_1 is the Legendre polynomial of rank 1, and $\hat{u}_i(t)$ is the unit dipole moment vector of the tagged component (IL cation/anion or water) at time t. The angular brackets denote that the calculations are carried out by averaging over all the tagged components at different initial reference times. We have considered the direction of $\hat{u}$ for the $BMIM^+$ cation along the direction perpendicular to the imidazolium ring center, while that for the SCN^- anion is taken as the direction perpendicular to the molecular axis. The directions of $\hat{u}$ for the other anions and water molecules are taken along the directions of the respective molecular dipolar axis.

The relaxations of the function $C_1(t)$ for the IL cation-anion components and water molecules near the surface of the protein (within 6 Å) in different aqueous IL solutions are shown in Figure 6. The corresponding result for water around the protein in pure aqueous medium in absence of any IL is included in the inset of Figure 6(c). For comparison, the relaxations of $C_1(t)$ for the IL components and water in different aqueous IL solutions in absence of the protein have been computed and presented in Figure S2 of the Supporting Information. As a reference, the data for pure bulk water is included in Figure S2(c) as inset. The errors associated with the data presented are found to vary within 3–4%. To further quantify the data, we have fitted the $C_1(t)$ relaxation curves with multi-exponentials (see eq. 4 with $N = 4$), and extracted the corresponding amplitude-weighted average reorientational relaxation times ($\langle\tau_\mu\rangle$). The $\langle\tau_\mu\rangle$ values for the cation-anion components of different ILs and water molecules at the interface, as well as that in respective bulk states are listed in Table 4. It is apparent from Figure 6 and Figure S2 that the presence of anions of different shapes and hydrophobic/hydrophilic characters leads to heterogeneously restricted reorientational

motions of the IL components and water. Presence of the protein molecule further enhances the extent of restriction on reorientational motions at the interface with significant increase in $\langle \tau_\mu \rangle$ values, as evident from the data. Such increasingly restricted reorientational motions of the IL components and water confined at the protein surface is in general consistent with their restricted diffusivity and significantly greater time scale of maximum dynamic heterogeneity, as discussed earlier (see Sections 3.2.1 and 3.3). It is apparent from Table 4 that the reorientational relaxation times for the $BMIM^+$ cations near the protein surface as well as in bulk solutions increase with increase in hydrophobic character of the anion component. The present calculation shows that the $\langle \tau_\mu \rangle$ value for the $BMIM^+$ cation in binary aqueous solution containing the most hydrophobic TF_2N^- anion is $\sim$8 times longer than that containing the most hydrophilic anion, SCN^-. Importantly, though the reorientations of the IL cations at the protein surface are more restricted, as evident from 4-12 times longer $\langle \tau_\mu \rangle$ values as compared to pure binary solutions, but their correlation with increased hydrophobicity of the anion component remains nearly the same. Interestingly, our calculation demonstrates that the relative trends among the heterogeneous reorientational time scales of the $BMIM^+$ cations and water molecules in presence of different anions are correlated with the corresponding trends associated with their translational diffusivity around the protein as well as in pure binary aqueous solutions (see Section 3.2.1). However, in contrast, the relative trends associated with the reorientational relaxation times of the anions have been found to be uncorrelated or anticorrelated with that observed with their diffusion time scales. It is apparent that besides the hydrophobic/hydrophilic character, the reorientational motion of an anion depends on its shape. SCN^- being linear and hydrophilic is expected to remain solvated with water molecules forming rigid cages around it. As a result though it diffuses on a much faster time scale as compared to the other anions, but it exhibits highly hindered reorientations within the solvation cage along directions perpendicular to its molecular axis, as evident from Figure 6 and Figure S2. Expectedly, the effect is more at the interface of

the protein as compared to bulk IL solutions. On the other hand, due to non-linear shape, greater flexibility and relatively enhanced hydrophobic character of the other anions considered (DCA^-, MS^-, TFO^- and TF_2N^-), the solvation around those are comparatively less rigid. As a result, compared to SCN^-, these anions exhibit relatively less hindered reorientations as evident from the corresponding $\langle\tau_\mu\rangle$ values. Interestingly, it can be further seen that the presence of the protein significantly alters the relaxation patterns of $C_1(t)$ for the anions (except SCN^-) confined at the interface (Figure 6) as compared to that in pure binary IL solutions (Figure S2). This is particularly evident for the most hydrophobic TF_2N^- anion. It is apparent that due to large size and hydrophobic nature, TF_2N^- diffuses on a slower time scale in pure solution, but it tends to reorient on a faster time scale as compared to all the other anions due to its inherent flexibility and non-linear shape. However, the effect of the protein on the degree of restriction of TF_2N^- reorientation is much higher as compared to DCA^-, MS^- and TFO^- as evident from the corresponding $\langle\tau_\mu\rangle$ values (Table 4). Such apparent anomaly in reorientational dynamics of different anions around the protein is likely to be correlated with their nonuniform interaction with the protein and the dynamics of hydrogen bond network at the interface. We discuss this in the next section.

3.5 Hydrogen Bond Network at the Interface

It is known that the presence of a protein in aqueous solution disrupts the regular water–water (WW) hydrogen bond network due to the formation of stronger protein–water (PW) hydrogen bonds at the interface.[61] PW hydrogen bonds play a critical role in controlling the structure, dynamics, and hence the functionality of the protein. It has been shown that the presence of an IL as co-solvent leads to further rearrangement of hydrogen bonding environment at the interface with the formation of protein-IL (PI) hydrogen bonds.[16,43] Several experimental and simulation studies have reported that such rearrangement perturbs the solvation environment around the protein with a direct consequence on its stability.[23,62–64]

Nonuniform translational and reorientational motions and the time scale of dynamic heterogeneity of the BMIM-based ILs and water molecules near the surface (within 6 Å) of the protein α-lactalbumin depending on the shapes/sizes and relative hydrophobic/hydrophilic characters of the anion components (A^-) as discussed earlier are expected to influence the relaxation time scale of hydrogen bonds at the interface. We explore such influence on the interfacial hydrogen bond dynamics in this section. It may be noted that the dynamics of hydrogen bonds can be studied indirectly and analyzed only qualitatively from experimental studies.[65,66] On the other hand, MD studies can provide quantitative information on hydrogen bond dynamics. For that, it is necessary to identify hydrogen bonds by using appropriate definitions. In this study, we have employed simple geometry-based criteria to define hydrogen bonds.[67,68] According to this, the first condition for a hydrogen bond to form is the distance between the tagged donor and acceptor sites be within 3.4 Å, while the second condition is that the angle between the hydrogen-donor-acceptor (H-D-A) be within 30°. Using these criteria, we have identified different types of hydrogen bonds at the interface along the simulated trajectories of the protein in different aqueous IL solutions, namely, the protein-$BMIM^+$ cation (PB), protein-anion (PA) and protein-water (PW) hydrogen bonds. Dynamics of these hydrogen bonds are then studied by calculating two well-known time correlation functions (TCFs), known as the intermittent ($C(t)$) and the continuous ($S(t)$) hydrogen bond TCFs.[69–71] These two functions are defined as

$$C(t) = \frac{\langle q(0)q(t)\rangle}{\langle q(0)q(0)\rangle} \tag{8}$$

and

$$S(t) = \frac{\langle q(0)Q(t)\rangle}{\langle q(0)q(0)\rangle} \tag{9}$$

where $q(t)$ and $Q(t)$ represent two different hydrogen bond population variables that can have two values, either zero or unity. The variable $q(t)$ becomes unity if a particular tagged

pair of sites are hydrogen bonded at a particular time t, and zero otherwise. The variable $Q(t)$, on the other hand, is unity when a tagged pair of sites are found to remain hydrogen bonded continuously from time $t = 0$ to a later time t. The results for a particular type of hydrogen bonds (PB, PA or PW) are obtained by averaging over all the hydrogen bonds of that type at different time origins. It may be noted that according to the above definitions, $C(t)$ describes the probability of finding a particular type of hydrogen bond formed at $t = 0$ to remain intact at a time t later. In other words, $C(t)$ takes into account recrossing of the barrier between the 'bound' and 'free' or 'quasi-free' states of the pair of hydrogen-bonded sites at intermediate times and their long-time diffusive behavior. Therefore, time evolution of $C(t)$ quantifies the time scale associated with the overall structural relaxation of hydrogen bonds. The function $S(t)$, on the other hand describes the probability of a particular hydrogen bond formed at $t = 0$ to remain continuously intact up to a time t later. Thus, $S(t)$ can provide a true measure of the lifetime or survival time of a particular type of hydrogen bond since its formation.

3.5.1 Intermittent Hydrogen Bond TCF

We have calculated the intermittent hydrogen bond TCFs, $C_{PB}(t)$, $C_{PA}(t)$ and $C_{PW}(t)$, for the PB, PA and PW hydrogen bonds formed between the protein residues and the IL components and water molecules present at the interface, the relaxations of which for different systems are displayed in Figure 7. For comparison, the corresponding result for PW hydrogen bonds around the protein in absence of any IL is included in Figure 7(c). The relative errors involved in the calculations are found to be rather small (within 1–2 %). To obtain a quantitative measure of the relaxation time scales of different hydrogen bonds at the interface, we have fitted the corresponding decay curves with triexponentials (eq. 4) and extracted the amplitude-weighted average relaxation times ($\langle\tau_C^{PB}\rangle$, $\langle\tau_C^{PA}\rangle$ and $\langle\tau_C^{PW}\rangle$), which are listed in Table 5. Our analysis showed that though there is a noticeable pop-

ulation of the $BMIM^+$ cation at the interface (Figure 1), but due to large size and rigid shape of the imidazolium ring, the probability of its hydrogen bond acceptor nitrogen (N) atoms to appropriately reorient and come within the hydrogen bond forming distance with the protein residues to form PB hydrogen bonds is rather small. Due to such geometrical constraints, only a small fraction of the $BMIM^+$ cations form PB hydrogen bonds which are transient in nature. This is true irrespective of the nature of the anions, and is evident from rapid relaxation of $C_{PB}(t)$ with $\langle \tau_C^{PB} \rangle$ values varying within 2–3 ps. In contrast, the dynamics of PA and PW hydrogen bonds at the interface have been found to be interesting. It is apparent from Figure 7(c) that the presence of an IL results in significantly slower relaxation of PW hydrogen bonds around the protein as compared to that in pure aqueous solution. Compared to the $\langle \tau_C^{PW} \rangle$ value of 42.1 ps in pure aqueous solution as obtained from our calculation, presence of different ILs near the protein surface leads to ∼2–3 times longer PW hydrogen bond relaxation times, as evident from Table 5. Such slower relaxation of PW hydrogen bonds at the interface is correlated with increasingly restricted diffusivity and longer residence times of water molecules at the interface in presence of ILs, as discussed before (see sections 3.2.1 and 3.2.2). Importantly, we find that the degree of hydrophobicity of the IL anions have influence on the relaxation time scale of PW hydrogen bonds. The calculation reveals that the relatively faster interfacial water motion in presence of the hydrophobic TF_2N^- anions as compared to the other ones as discussed in Section 3.2.1 is associated with faster PW hydrogen bond relaxation. Table 5 reveals that the PW hydrogen bonds in presence of TF_2N^- anions relax on a time scale 15–30 % shorter as compared to that in presence of other anions. Importantly, Figure 7(b) reveals significantly heterogeneous relaxation of PA hydrogen bonds involving different IL anions. The degree of such heterogeneity depends on the relative hydrophobic/hydrophilic character of the anion considered. Increasingly restricted diffusivity with a consequent longer residence time at the interface with increased hydrophobicity of the anions as observed earlier (see sections 3.2.1 and 3.2.2)

has been found to be largely correlated with the time scale of PA hydrogen bond relaxations. For example, the PA hydrogen bonds formed by the hydrophobic TF_2N^- anions are found to relax on a much longer time scale with 12–48 % greater $\langle \tau_C^{PW} \rangle$ value as compared to that involving the other less hydrophobic anions studied.

3.5.2 Continuous Hydrogen Bond TCF

The relaxations of the continuous hydrogen bond TCFs for the PB, PA and PW hydrogen bonds at the surface of the protein ($S_{PB}(t)$, $S_{PA}(t)$ and $S_{PW}(t)$) are depicted in Figure 8. As a reference, the corresponding result for the PW hydrogen bonds around the protein in absence of any IL is included in Figure 8(c). It may be noted that for appropriate sampling of these TCFs, the trajectory blocks (see Section 2) were rerun and stored with a higher time resolution of 10 fs. The estimated errors involved in the calculations are found to be within 3 %. As mentioned before (eq. 9), relaxation behavior of $S(t)$ provides a direct estimate of the lifetime of a hydrogen bond. We have fitted the decay curves corresponding to the PB, PA and PW hydrogen bonds around the protein in presence of different ILs with tri-exponentials (eq. 4) and extracted the average lifetimes ($\langle \tau_S^{PB} \rangle$, $\langle \tau_S^{PA} \rangle$ and $\langle \tau_S^{PW} \rangle$), which are listed in Table 6. As discussed in the previous section, due to geometrical constraints, the imidazolium ring of the $BMIM^+$ cation cannot orient appropriately at the protein surface to form PB hydrogen bonds. As a result, the PB hydrogen bonds are transient in nature with breaking and reformation occurring on a much faster time scale. This is evident from extremely rapid decay of $S_{PB}(t)$ with the average lifetimes ($\langle \tau_S^{PB} \rangle$) varying within 100 fs. Irrespective of the nature of the anion component, presence of an IL as co-solvent leads to relatively slower relaxation of $S_{PW}(t)$ for the PW hydrogen bonds at the protein surface as compared to that in pure aqueous medium, as evident from Figure 8(c). This is consistent with the relaxation patterns of $C_{PW}(t)$, as discussed before (Figure 7(c)). Except for the IL containing TF_2N^- anion for which the PW hydrogen bond relaxation is close to that in

pure aqueous medium, the effect has been found to be more and nearly uniform for other aqueous IL solutions. The data presented in Table 6 show that compared to the $\langle \tau_S^{PW} \rangle$ value of 1.52 ps in pure aqueous solution as obtained from our calculation, presence of different ILs near the protein surface leads to 20–60 % longer lifetimes of PW hydrogen bonds. Note that the lifetime of a particular hydrogen bond should depend on its strength, as a stronger hydrogen bond is expected to survive longer and vice versa. We have calculated the average strength of a PW hydrogen bond ($\langle E_{PW} \rangle$), defined as the interaction energy between an amino acid residue of the protein and a water molecule with which it is hydrogen bonded. The calculation shows that the PW hydrogen bonds formed at the interface in presence of the ILs are marginally stronger with $\langle E_{PW} \rangle$ values varying within –9 to –10 kcal mol^{-1}, as compared to the $\langle E_{PW} \rangle$ value of –8 kcal mol^{-1} in pure water. Thus, it is clear that the formation of marginally stronger PW hydrogen bonds at the interface in presence of the ILs is the origin behind their relatively longer lifetimes.

Compared to the PB and PW hydrogen bonds, significantly heterogeneous relaxation of $S_{PA}(t)$ for the PA hydrogen bonds involving the IL anions of different shapes/sizes and varying degree of hydrophobicity is evident from Figure 8(b). Interestingly, comparison of the present result with that presented in Figure 7(b) reveals that the relaxation patterns of $S_{PA}(t)$ among different anions at the interface are anticorrelated with that of $C_{PA}(t)$. This is particularly evident for the most hydrophilic and hydrophobic anions, namely, SCN^- and TF_2N^-, respectively. It can be seen that though the overall structural relaxation of PA hydrogen bonds formed by the SCN^- ions at the interface occur on a relatively short time scale, but their average lifetime is maximum among different anions. Reverse trend has been observed for the hydrophobic TF_2N^- anions. Long-time structural relaxation of PA hydrogen bonds formed by the TF_2N^- anions (Figure 7(b)) is associated with their shorter lifetimes. It is apparent from Table 6, that the average lifetime of 3.21 ps for the PA hydrogen bonds formed by the SCN^- anions ($\langle \tau_S^{PA} \rangle$) is 2–6 times longer as compared to

that formed by the other anions. To probe the origin behind such contrasting dynamics of PA hydrogen bonds at the interface, we have calculated the average PA hydrogen bond strength ($\langle E_{PA} \rangle$), defined as the interaction energy between a protein residue and an IL anion with which it is hydrogen bonded. It is found that the average strength of a PA hydrogen bond formed by SCN^- anion is –33.4 kcal mol^{-1}, while that for PA hydrogen bonds involving other anions vary within –11 to –16 kcal mol^{-1}. Greater PA hydrogen bond strength formed by SCN^- as observed in the present study is consistent with earlier work,[72] where it was demonstrated that SCN^- exhibits strong propensity to break weaker PW hydrogen bonds by much stronger PA hydrogen bonds. It is clear from our study that significantly longer lifetimes of PA hydrogen bonds formed by SCN^- originates from its ability to form much stronger hydrogen bonds with the protein at the interface. We discussed earlier (Section 3.4) that due to strong hydrophilic nature, SCN^- anions are surrounded by rigid solvent cages, thereby causing their hindered reorientations. The present result demonstrates that in addition to rigid solvent cages, formation of strong PA hydrogen bonds at the interface also contributes toward significantly restricted reorientation time scale of SCN^- anions as compared to the other anions studied. Finally, it may be noted that a hydrogen bond being directional in nature, proper orientation of the two sites are important for its formation. Though, TF_2N^- anion have maximum number of hydrogen bond acceptor sites, but due to geometrical constraints it cannot orient appropriately at the interface to form PA hydrogen bonds. As a result, they form weaker PA hydrogen bonds at the interface ($\langle E_{PA} \rangle$ value of –11 kcal mol^{-1}) and hence have shorter lifetimes. Importantly, due to slower translational diffusivity and longer residence times at the interface (Figures 2 and 3), propensity of reformation rates of broken PA hydrogen bonds is expected to be higher for the hydrophobic TF_2N^- anions at the protein surface as compared to the hydrophilic anions, such as SCN^-. Further studies are under progress in our laboratory to explore this aspect in greater details.

4 CONCLUSIONS

In this study we have carried out comprehensive room temperature MD simulations of the protein α-lactalbumin in 2M binary aqueous solutions of BMIM-based ILs with a series of different Hofmeister anions based on their hydrophobicity, namely, SCN^-, DCA^-, MS^-, TFO^- and TF_2N^-. Attempts have been made to explore the effects of different shapes/sizes and hydrophobic/hydrophilic characters of the anions on the heterogeneous dynamic environment at the interface around the protein. The results are compared with that of the protein in pure water as well as that of pure binary IL solutions at identical concentration.

Our calculations revealed exchange of population between water and IL cation-anion pairs beyond the first layer of bound water molecules at the protein surface. Due to differential shapes and sizes of the anions, the distributions of the cation-anion pairs around the protein have been found to be nonuniform. Such nonuniform distribution of IL components near the protein are found to modify the dynamic environment at the interface in a heterogeneous manner. The results demonstrated that in addition to increasingly restricted water motion at the interface, the presence of the protein leads to further restricted diffusivity of the IL ion pairs around it as compared to pure aqueous IL solutions, the degree of restriction being more in presence of the hydrophobic anions (TF_2N^-). In contrast, due to relatively weaker hydration, water molecules in presence of a slower hydrophobic IL (e.g., [BMIM][TF_2N]) exhibit relatively faster dynamics as compared to water molecules that are strongly hydrated in presence of an hydrophilic IL (e.g., [BMIM][SCN]). The extent of such contrasting diffusion time scales between the IL components and water are more evident at the interface around the protein. The calculation further quantifies how the increasingly restricted diffusivity of the IL components and water around the protein is associated with longer time scale for the onset of dynamic heterogeneity at the interface. Interestingly, in contrast to the $BMIM^+$ cations and water, the reorientational relaxation time scale of the anions are found

to be anticorrelated with their translational diffusivity both in binary aqueous solutions and around the protein, the effect being more at the interface. It is found that SCN^- ions being linear and hydrophilic with strong hydrogen bond forming ability with water form rigid solvation cages around them. As a result, though the SCN^- ions diffuse on a faster time scale, but they exhibit highly hindered reorientations within their solvation cages as compared to the other IL anions. Interestingly, an anomalous effect of confinement near the protein surface on the reorientational motions of hydrophobic anions (such as TF_2N^-) have been observed. It is noticed that due to non-linear shape and greater inherent flexibility, TF_2N^- ions tend to reorient on a faster time scale as compared to the other anions in pure aqueous solution. However, presence of the protein significantly restricts such inherent flexibility, thereby leading to much slower reorientations of TF_2N^- ions at the interface as compared to most of the other anions (except SCN^-). Importantly, the calculation demonstrated that the increasingly restricted diffusivity and longer residence times of water molecules at the interface in presence of the ILs are correlated with significantly slower structural relaxations of protein-water (PW) hydrogen bonds around the protein. Further, in addition to the diffusivity time scale, the relative hydrophobic/hydrophilic characters of the anions are found to play important roles in defining the relaxation time scale of the protein-anion (PA) hydrogen bonds. The calculation revealed that compared to pure aqueous medium, presence of an IL allows the protein to form relatively stronger PW hydrogen bonds with longer lifetimes at the interface. More importantly, it is found that though the overall structural relaxation of PA hydrogen bonds formed by the hydrophilic SCN^- ions at the interface occur on a relatively shorter time scale, but they form much stronger PA hydrogen bonds with maximum lifetime among different ions. Reverse trend has been observed for the hydrophobic TF_2N^- anions. The PA hydrogen bonds formed by the TF_2N^- anions are relatively weaker with shorter lifetimes though their structural relaxation occur on longer time scale.

5 ACKNOWLEDGMENTS

This study was supported by grant received from the Science and Engineering Research Board (SERB) under the Department of Science and Technology (DST), Government of India (Ref. No. CRG/2020/000044). Krishna P. Ghanta thank Council of Scientific and Industrial Research (CSIR), Government of India (09/081(1312)/2017-EMR-I, dated 18.10.2017 and Sandip Mondal thanks University Grants Commission (UGC), Government of India (23/12/2012(ii)EU-V) for providing scholarships. This work used the resources of the Supercomputing facility of the Indian Institute of Technology Kharagpur established under National Supercomputing Mission (NSM), Government of India and supported by the Centre for Development of Advanced Computing (CDAC), Pune.

6 Associated Content

Supporting Information Available

The Supporting Information is available free of charge on the ACS publication website at DOI:

Table S1: Average numbers of the IL cations (N_{BMIM^+}), different anions (N_{A^-}) and water molecules (N_W) present at the protein interface (within 6 Å) in different systems. Average number of water molecules around the protein in absence of any IL is listed for comparison. Figure S1: Mean square displacements (MSD) of (a) $BMIM^+$ cations (b) different anions (A^-) and (c) water molecules in different bulk aqueous IL solutions in absence of the protein. The corresponding diffusion coefficient (D_E) values are shown in the insets. As a reference, MSD of water in pure bulk state is included in (c). Figure S2: Relaxations of the reorientational time correlation function ($C_1(t)$) for (a) $BMIM^+$ cations (b) different anions (A^-) and (c) water molecules in different aqueous IL solutions in absence of the protein. As a reference, the corresponding data for water in pure bulk state is included as inset in (c).

References

(1) Veprintsev, D. B.; Permyakov, S. E.; Permyakov, E. A.; Rogov, V. V.; Cawthern, K. M.; Berliner, L. J. Cooperative Thermal Transitions of Bovine and Human apo-α-Lactalbumins: Evidence for a New Intermediate State. *FEBS Lett.* **1997**, *412*, 625–628.

(2) Stacey, A.; Schnieke, A.; Kerr, M.; Scott, A.; McKee, C.; Cottingham, I.; Binas, B.; Wilde, C.; Colman, A. Lactation is Disrupted by Alpha-Lactalbumin Deficiency and can be Restored by Human Alpha-Lactalbumin Gene Replacement in Mice. *Proc. Natl. Acad. Sci. U.S.A* **1995**, *92*, 2835–2839.

(3) Fischer, W.; Gustafsson, L.; Mossberg, A.-K.; Gronli, J.; Mork, S.; Bjerkvig, R.; Svanborg, C. Human α-Lactalbumin Made Lethal to Tumor Cells (HAMLET) Kills Human Glioblastoma Cells in Brain Xenografts by an Apoptosis-Like Mechanism and Prolongs Survival. *Cancer Res.* **2004**, *64*, 2105–2112.

(4) Galiński, M.; Lewandowski, A.; Stepniak, I. Capacitive Energy Storage in Nanostructured Carbon–Electrolyte Systems. *Electrochim. Acta* **2006**, *51*, 5567.

(5) Andriyko, Y. O.; Reischl, W.; Nauer, G. E. Trialkyl-Substituted Imidazolium-Based Ionic Liquids for Electrochemical Applications: Basic Physicochemical Properties. *J. Chem. Eng. Data* **2009**, *54*, 855–860.

(6) Constantinescu, D.; Weingärtner, H.; Herrmann, C. Protein Denaturation by Ionic Liquids and the Hofmeister Series: A Case Study of Aqueous Solutions of Rribonuclease A. *Angew. Chem. Int. Ed.* **2007**, *46*, 8887–8889.

(7) Baker, G. A.; Heller, W. T. Small-Angle Neutron Scattering Studies of Model Protein

Denaturation in Aqueous Solutions of the Ionic Liquid 1-Butyl-3-Methylimidazolium Chloride. *Chem. Eng. J.* **2009**, *147*, 6–12.

(8) Yang, Z.; Pan, W. Ionic Liquids: Green Solvents for Nonaqueous Biocatalysis. *Enzyme Microb. Technol.* **2005**, *37*, 19–28.

(9) van Rantwijk, F.; Sheldon, R. A. Biocatalysis in Ionic Liquids. *Chem. Rev.* **2007**, *107*, 2757–2785.

(10) Sankaranarayanan, K.; Dhathathreyan, A.; Kragel, J.; Miller, R. Interfacial Viscoelasticity of Myoglobin at Air/Water and Air/Solution Interfaces: Role of Folding and Clustering. *J. Phys. Chem. B* **2012**, *116*, 895–902.

(11) Fujita, K.; Ohno, H. Enzymatic Activity and Thermal Stability of Metallo Proteins in Hydrated Ionic Liquids. *Biopolymers* **2010**, *93*, 1093–1099.

(12) Schindl, A.; Hagen, M. L.; Muzammal, S.; Gunasekera, H. A.; Croft, A. K. Proteins in Ionic Liquids: Reactions, Applications, and Futures. *Front. Chem.* **2019**, *7*, 347.

(13) Shukla, S. K.; Mikkola, J.-P. Use of Ionic Liquids in Protein and DNA Chemistry. *Front. Chem.* **2020**, *8*, 1219.

(14) Schröder, C. Proteins in Ionic Liquids: Current Status of Experiments and Simulations. *Top. Curr. Chem.* **2017**, *375*, 25.

(15) Nordwald, E. M.; Armstrong, G. S.; Kaar, J. L. NMR-Guided Rational Engineering of an Ionic-Liquid-Tolerant Lipase. *ACS Catal.* **2014**, *4*, 4057–4064.

(16) Shao, Q. On the Influence of Hydrated Imidazolium-Based Ionic Liquid on Protein Structure Stability: a Molecular Dynamics Simulation Study. *J. Chem. Phys.* **2013**, *139*, 115102.

(17) Figueiredo, A. M.; Sardinha, J.; Moore, G. R.; Cabrita, E. J. Protein Destabilisation in Ionic Liquids: The Role of Preferential Interactions in Denaturation. *Phys. Chem. Chem. Phys.* **2013**, *15*, 19632–19643.

(18) Tung, H.-J.; Pfaendtner, J. Kinetics and Mechanism of Ionic-Liquid Induced Protein Unfolding: Application to the Model Protein HP35. *Mol. Syst. Des. Eng.* **2016**, *1*, 382–390.

(19) Bui-Le, L.; Clarke, C. J.; Bröhl, A.; Brogan, A. P.; Arpino, J. A.; Polizzi, K. M.; Hallett, J. P. Revealing the Complexity of Ionic Liquid–Protein Interactions Through a Multi-Technique Investigation. *Commun. Chem.* **2020**, *3*, 1–9.

(20) Alves, M. M.; Araújo, J. M.; Martins, I. C.; Pereiro, A. B.; Archer, M. Insights into the Interaction of Bovine Serum Albumin with Surface-Active Ionic Liquids in Aqueous Solution. *J. Mol. Liq.* **2021**, *322*, 114537.

(21) Klähn, M.; Lim, G. S.; Wu, P. How Ion Properties Determine the Stability of a Lipase Enzyme in Ionic Liquids: A Molecular Dynamics Study. *Phys. Chem. Chem. Phys.* **2011**, *13*, 18647–18660.

(22) Piccoli, V.; Martinez, L. Correlated Counterion Effects on the Solvation of Proteins by Ionic Liquids. *J. Mol. Liq.* **2020**, *320*, 114347.

(23) Haberler, M.; Schröder, C.; Steinhauser, O. Hydrated Ionic Liquids with and without Solute: The Influence of water Content and Protein Solutes. *J. Chem. Theory Comput.* **2012**, *8*, 3911–3928.

(24) Haberler, M.; Schröder, C.; Steinhauser, O. Solvation Studies of a Zinc Finger Protein in Hydrated Ionic Liquids. *Phys. Chem. Chem. Phys.* **2011**, *13*, 6955–6969.

(25) Kumar, A.; Venkatesu, P. Does the Stability of Proteins in Ionic Liquids Obey the Hofmeister Series? *Int. J. Biol. Macromol.* **2014**, *63*, 244–253.

(26) Galamba, N. Mapping Structural Perturbations of Water in Ionic Solutions. *J. Phys. Chem. B* **2012**, *116*, 5242–5250.

(27) Collins, K. D.; Washabaugh, M. W. The Hofmeister Effect and the Behaviour of Water at Interfaces. *Q. Rev. Biophys.* **1985**, *18*, 323–422.

(28) Ries-Kautt, M.; Ducruix, A. F. Relative Effectiveness of Various Ions on the Solubility and Crystal Growth of Lysozyme. *J. Biol. Chem* **1989**, *264*, 745–748.

(29) Finet, S.; Skouri-Panet, F.; Casselyn, M. F. Bonnete; A. Tardieu. *Curr. Opin. Colloid Interface Sci.* **2004**, *9*, 112.

(30) Nordwald, E. M.; Kaar, J. L. Stabilization of Enzymes in Ionic Liquids via Modification of Enzyme Charge. *Biotechnol. Bioeng* **2013**, *110*, 2352–2360.

(31) Timasheff, S. N. Protein-Solvent Preferential Interactions, Protein Hydration, and the Modulation of Biochemical Reactions by Solvent Components. *Proc. Natl. Acad. Sci. U.S.A.* **2002**, *99*, 9721–9726.

(32) Abraham, M. J.; Murtola, T.; Schulz, R.; Páll, S.; Smith, J. C.; Hess, B.; Lindahl, E. GROMACS: High Performance Molecular Simulations Through Multi-Level Parallelism from Laptops to Supercomputers. *SoftwareX* **2015**, *1*, 19–25.

(33) Pike, A. C.; Brew, K.; Acharya, K. R. Crystal Structures of Guinea-Pig, Goat and Bovine A-Lactalbumin Highlight the Enhanced Conformational Flexibility of Regions that are Significant for its Action in Lactose Synthase. *Structure* **1996**, *4*, 691–703.

(34) Jorgensen, W. L.; Maxwell, D. S.; Tirado-Rives, J. Development and Testing of the OPLS All-Atom Force Field on Conformational Energetics and Properties of Organic Liquids. *J. Am. Chem. Soc.* **1996**, *118*, 11225–11236.

(35) Doherty, B.; Zhong, X.; Gathiaka, S.; Li, B.; Acevedo, O. Revisiting OPLS Force Field Parameters For Ionic Liquid Simulations. *J. Chem. Theory .Comput.* **2017**, *13*, 6131–6145.

(36) Jorgensen, W. L.; Chandrasekhar, J.; Madura, J. D.; Impey, R. W.; Klein, M. L. Comparison of Simple Potential Functions for Simulating Liquid Water. *J. Chem. Phys.* **1983**, *79*, 926–935.

(37) Martínez, L.; Andrade, R.; Birgin, E. G.; Martínez, J. M. PACKMOL: A Package for Building Initial Configurations for Molecular Dynamics Simulations. *J. Comput. Chem.* **2009**, *30*, 2157–2164.

(38) Hess, B.; Bekker, H.; Berendsen, H. J.; Fraaije, J. G. LINCS: A Linear Constraint Solver for Molecular Simulations. *J. Comput. Chem.* **1997**, *18*, 1463–1472.

(39) Berendsen, H. HJC Berendsen, JPM Postma, WF van Gunsteren, A. DiNola, and JR Haak, J. Chem. Phys. 81, 3684 (1984). *J. Chem. Phys.* **1984**, *81*, 3684.

(40) Bussi, G.; Donadio, D.; Parrinello, M. Canonical Sampling Through Velocity Rescaling. *J. Chem. Phys.* **2007**, *126*, 014101.

(41) Feller, S. E.; Zhang, Y.; Pastor, R. W.; Brooks, B. R. Constant Pressure Molecular Dynamics Simulation: The Langevin Piston Method. *J. Chem. Phys.* **1995**, *103*, 4613–4621.

(42) Darden, T.; York, D.; Pedersen, L. Particle Mesh Ewald: An N log (N) Method for Ewald sums in Large Systems. *J. Chem. Phys.* **1993**, *98*, 10089–10092.

(43) Ghanta, K. P.; Mondal, S.; Mondal, S.; Bandyopadhyay, S. Contrasting Effects of Ionic Liquids of Varying Degree of Hydrophilicity on the Conformational and Interfacial Properties of a Globular Protein. *J. Phys. Chem. B* **2021**, *125*, 9441–9453.

(44) Astley, T.; Birch, G. G.; Drew, M. G.; Rodger, P. M.; Wilden, G. R. Effect of Available Volumes on Radial Distribution Functions. *J. Comput. Chem.* **1998**, *19*, 363–367.

(45) Allen, M. P.; Tildesley, D. J. *Computer Simulation of Liquids*; Oxford university press, 1987.

(46) Tokuda, H.; Tsuzuki, S.; Susan, M. A. B. H.; Hayamizu, K.; Watanabe, M. How Ionic are Room-Temperature Ionic Liquids? An Indicator of the Physicochemical Properties. *J. Phys. Chem. B* **2006**, *110*, 19593–19600.

(47) Bizzarri, A. R.; Cannistraro, S. Molecular Dynamics of Water at the Protein- Solvent Interface. 2002.

(48) Sinha, S. K.; Bandyopadhyay, S. Local Heterogeneous Dynamics of Water Around Lysozyme: A Computer Simulation Study. *Phys. Chem. Chem. Phys.* **2012**, *14*, 899–913.

(49) Chandra, A. Effects of ion Atmosphere on Hydrogen-Bond Dynamics in Aqueous Electrolyte Solutions. *Phys. Rev. Lett.* **2000**, *85*, 768–771.

(50) Liu, H.; Maginn, E. A Molecular Dynamics Investigation of the Structural and Dynamic Properties of the Ionic Liquid 1-n-butyl-3-methylimidazolium bis (trifluoromethanesulfonyl) imide. *J. chem. phys.* **2011**, *135*, 124507.

(51) Sengupta, B.; Yadav, R.; Sen, P. Startling Temperature Effect on Proteins when Confined: Single Molecular Level Behaviour of Human Serum Albumin in a Reverse Micelle. *Phys. Chem. Chem. Phys.* **2016**, *18*, 14350–14358.

(52) Bhargava, B.; Balasubramanian, S. Refined Potential Model for Atomistic Simulations of Ionic Liquid [bmim][PF 6]. *J. chem. phys.* **2007**, *127*, 114510.

(53) Pal, T.; Biswas, R. Composition Dependence of Dynamic Heterogeneity Time-and Length Scales in [Omim][BF4]/water Binary Mixtures: Molecular Dynamics Simulation Study. *J. Phys. Chem. B* **2015**, *119*, 15683–15695.

(54) Rahman, A. Correlations in the Motion of Atoms in Liquid Argon. *Phys. rev.* **1964**, *136*, A405–A411.

(55) Faupel, F.; Frank, W.; Macht, M.-P.; Mehrer, H.; Naundorf, V.; Rätzke, K.; Schober, H. R.; Sharma, S. K.; Teichler, H. Diffusion in Metallic Glasses and Supercooled Melts. *Rev. Mod. Phys.* **2003**, *75*, 237.

(56) Hansen, J.-P.; McDonald, I. R. *Theory of Simple Liquids*; Elsevier, 1990.

(57) Kob, W.; Donati, C.; Plimpton, S. J.; Poole, P. H.; Glotzer, S. C. Dynamical Heterogeneities in a Supercooled Lennard-Jones Liquid. *Phys. Rev. Lett.* **1997**, *79*, 2827.

(58) Shell, M. S.; Debenedetti, P. G.; Stillinger, F. H. Dynamic Heterogeneity and non-Gaussian Behaviour in a Model Supercooled Liquid. *J. Phys.: Condens. Matter* **2005**, *17*, S4035.

(59) Reddy, T. D. N.; Mallik, B. S. Heterogeneity in the Microstructure and Dynamics of Tetraalkylammonium Hydroxide Ionic Liquids: Insight from Classical Molecular Dynamics Simulations and Voronoi Tessellation Analysis. *Phys. Chem. Chem. Phys.* **2020**, *22*, 3466–3480.

(60) Sharma, A.; Ghorai, P. K. Effect of Water on Structure and Dynamics of [BMIM][PF6] Ionic Liquid: An All-atom Molecular Dynamics Simulation Investigation. *J. Chem. Phys.* **2016**, *144*, 114505.

(61) Bandyopadhyay, S.; Chakraborty, S.; Bagchi, B. Secondary Structure Sensitivity of Hydrogen Bond Lifetime Dynamics in the Protein Hydration Layer. *J. Am. Chem. Soc.* **2005**, *127*, 16660–16667.

(62) Bharmoria, P.; Kumar, A. Thermodynamic Investigations of Protein's Behaviour with Ionic Liquids in Aqueous Medium Studied by Isothermal Titration Calorimetry. *Biochim. Biophys. Acta, Gen. Subj.* **2016**, *1860*, 1017–1025.

(63) Jha, I.; Venkatesu, P. Unprecedented Improvement in the Stability of Hemoglobin in the Presence of Promising Green Solvent 1-allyl-3-methylimidazolium Chloride. *ACS Sustainable Chem. Eng.* **2016**, *4*, 413–421.

(64) Jaeger, V. W.; Pfaendtner, J. Structure, Dynamics, and Activity of Xylanase Solvated in Binary Mixtures of Ionic Liquid and Water. *ACS Chem. Biol.* **2013**, *8*, 1179–1186.

(65) Chen, S.; Teixeira, J. Structure and Dynamics of Low-Temperature Water as Studied by Scattering Techniques. *Adv. Chem. Phys* **1986**, *64*.

(66) Kropman, M.; Bakker, H. Dynamics of Water Molecules in Aqueous Solvation Shells. *Science* **2001**, *291*, 2118–2120.

(67) Forrest, J.; Svanberg, C.; Révész, K.; Rodahl, M.; Torell, L.; Kasemo, B. Phys Rev E: Stat Phys Plasmas Fluids Relat Interdiscip Top 1998, 58. *R1226*

(68) Rabideau, B. D.; Ismail, A. E. Mechanisms of Hydrogen Bond Formation Between Ionic Liquids and Cellulose and the Influence of Water Content. *Phys. Chem. Chem. Phys.* **2015**, *17*, 5767–5775.

(69) Stillinger, F. H. Theory and Molecular Models for Water. *Adv. Chem. Phys.* **1975**, 1–101.

(70) Stillinger, F. H. Water Revisited. *Science* **1980**, *209*, 451–457.

(71) Rapaport, D. Hydrogen Bonds in Water: Network Organization and Lifetimes. *Mol. Phys.* **1983**, *50*, 1151–1162.

(72) Kim, H.; Park, S.; Cho, M. Rotational Dynamics of Thiocyanate Ions in Highly Concentrated Aqueous Solutions. *Phys. Chem. Chem. Phys.* **2012**, *14*, 6233–6240.

Table 1: Total Numbers of the IL Cations/Anions ($N^{tot}_{BMIM^+}/N^{tot}_{A^-}$) and Water Molecules ($N^{tot}_W$) in Different Systems of 2M Concentration

system	$N^{tot}_{BMIM^+}/N^{tot}_{A^-}$	N^{tot}_W
[BMIM][SCN]	363	6160
[BMIM][DCA]	363	5925
[BMIM][MS]	363	5550
[BMIM][TFO]	363	5580
[BMIM][TF_2N]	363	4385

Table 2: Average Residence Times ($\langle\tau_R\rangle$) of the $BMIM^+$ Cations, Different Anions (A^-) and Water Molecules Present at the Protein Interface (Within 6 Å) in Different Systems

system	$\langle\tau_R\rangle$ (ps)		
	$BMIM^+$	A^-	water
[BMIM][SCN]	805.06	141.16	91.16
[BMIM][DCA]	633.88	343.08	92.12
[BMIM][MS]	1283.82	808.72	110.66
[BMIM][TFO]	945.70	956.18	127.64
[BMIM][TF_2N]	1731.33	1333.35	89.09

Table 3: Average Times Associated with Maximum Dynamic Heterogeneity ($\langle\tau_D\rangle$) for the $BMIM^+$ Cations, Different Anions (A^-) and Water Molecules Present at the Protein Interface (Within 6 Å) in Different Systems. The Corresponding Data for Bulk Aqueous IL Solutions are Listed for Comparison.

	interface ($\langle\tau_D\rangle$ (ps))			bulk ($\langle\tau_D\rangle$ (ps))		
system	$BMIM^+$	A^-	water	$BMIM^+$	A^-	water
[BMIM][SCN]	375	598	410	5.20	6.8	2.0
[BMIM][DCA]	925	360	315	20.4	39.6	1.6
[BMIM][MS]	279	200	327	108.0	171.6	1.6
[BMIM][TFO]	412	345	276	156.4	194.4	1.6
[BMIM][TF_2N]	1764	1152	334	410.8	198.0	1.2

Table 4: Average Reorientational Relaxation Times ($\langle\tau_\mu\rangle$) for the $BMIM^+$ Cations, Different Anions (A^-) and Water Molecules Present at the Protein Interface (Within 6 Å) in Different Systems. The Corresponding Data for Bulk Aqueous IL Solutions and That for Water Around the Protein in Absence of any IL are Listed for Comparison.

	interface ($\langle\tau_\mu\rangle$ (ps))			bulk ($\langle\tau_\mu\rangle$ (ps))		
system	$BMIM^+$	A^-	water	$BMIM^+$	A^-	water
[BMIM][SCN]	385.35	1025.74	47.19	58.53	109.02	10.63
[BMIM][DCA]	752.83	92.61	50.58	59.92	5.55	7.88
[BMIM][MS]	1050.27	86.99	59.32	127.74	7.62	8.67
[BMIM][TFO]	1108.40	435.73	58.43	149.69	97.40	8.77
[BMIM][TF_2N]	1727.74	575.57	45.18	457.56	4.51	9.62
aqueous medium (without IL)			27.99			2.23

Table 5: Average Relaxation Times ($\langle\tau_C^{PB}\rangle$, $\langle\tau_C^{PA}\rangle$, $\langle\tau_C^{PW}\rangle$) as Obtained from the Intermittent Hydrogen Bond Time Correlation Functions for the PB, PA and PW Hydrogen Bonds Formed at the Protein Interface

system	$\langle\tau_C^{PB}\rangle$ (ps)	$\langle\tau_C^{PA}\rangle$ (ps)	$\langle\tau_C^{PW}\rangle$ (ps)
[BMIM][SCN]	2.32	121.88	95.44
[BMIM][DCA]	2.67	172.51	104.71
[BMIM][MS]	2.89	119.93	96.21
[BMIM][TFO]	2.65	101.82	109.44
[BMIM][TF_2N]	3.39	196.15	83.10

Table 6: Average Relaxation Times ($\langle\tau_S^{PB}\rangle$, $\langle\tau_S^{PA}\rangle$, $\langle\tau_S^{PW}\rangle$) as Obtained from the Continuous Hydrogen Bond Time Correlation Functions for the PB, PA and PW Hydrogen Bonds Formed at the Protein Interface

system	$\langle\tau_S^{PB}\rangle$ (ps)	$\langle\tau_S^{PA}\rangle$ (ps)	$\langle\tau_S^{PW}\rangle$ (ps)
[BMIM][SCN]	0.063	3.21	2.29
[BMIM][DCA]	0.084	1.19	2.50
[BMIM][MS]	0.061	0.93	2.27
[BMIM][TFO]	0.057	1.33	2.31
[BMIM][TF_2N]	0.084	0.56	1.85

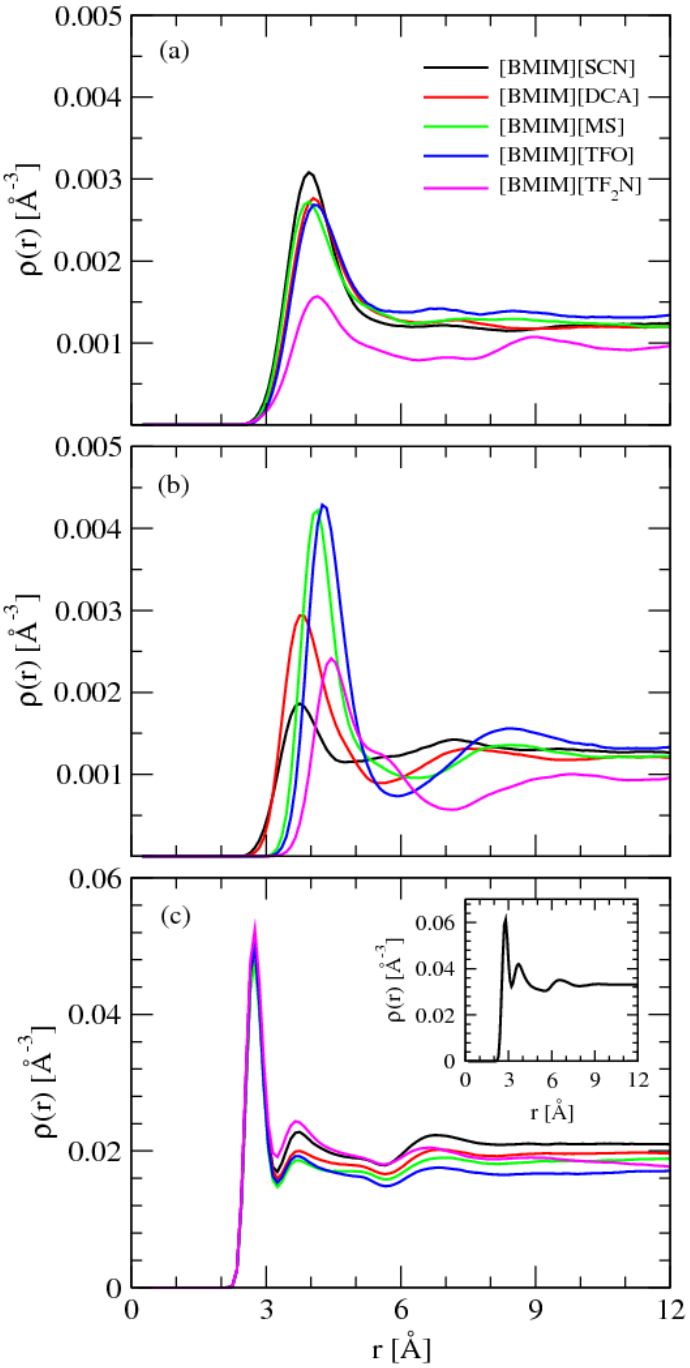

Figure 1: Number density profiles (ρ (r)) of (a) $BMIM^+$ cations; (b) different anions (A^-) and (c) water molecules as a function of distance from the protein surface for different systems. The corresponding data for water around the protein in pure aqueous medium in absence of any IL is shown as inset in (c).

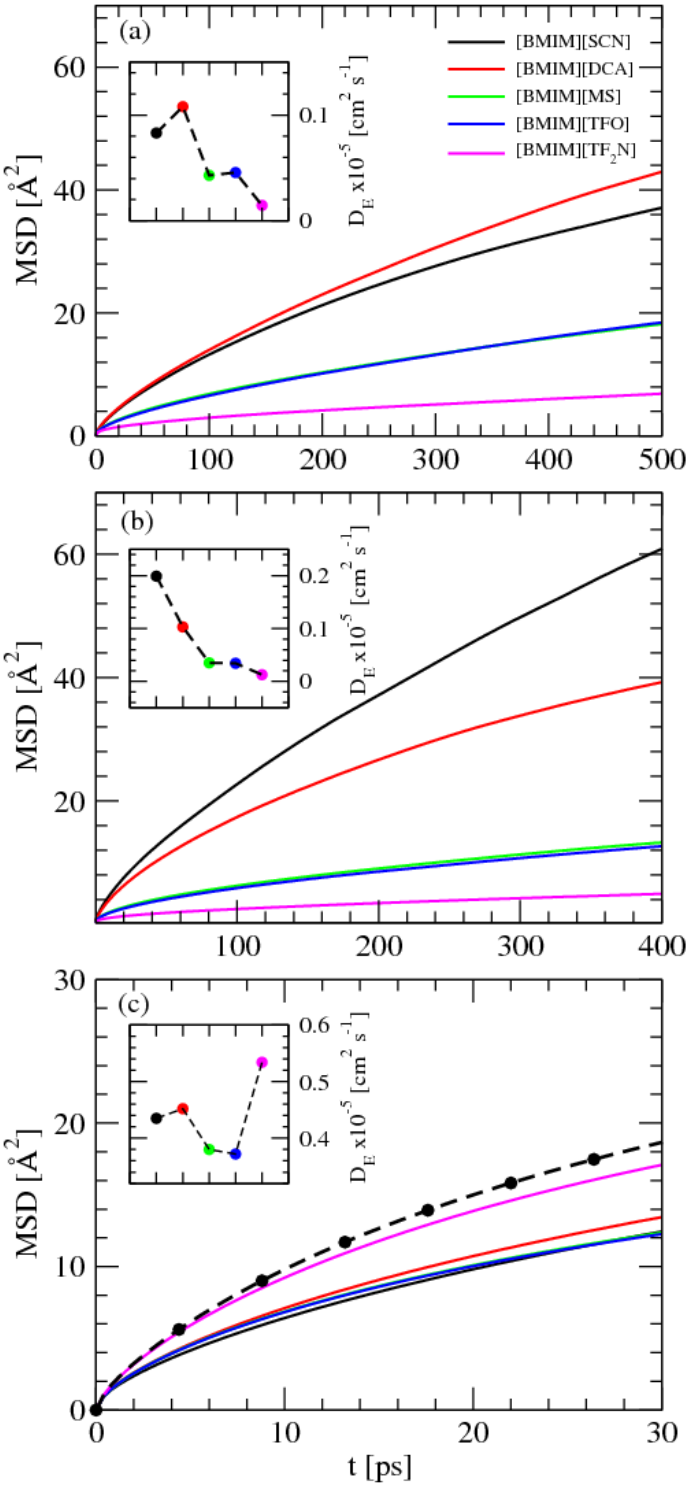

Figure 2: Mean square displacements (MSD) of (a) $BMIM^+$ cations; (b) different anions (A^-) and (c) water molecules present at the protein interface (within 6 Å) in different systems. The corresponding diffusion coefficient (D_E) values are shown in the insets. As a reference, MSD of water around the protein in pure aqueous medium in absence of any IL is included in (c).

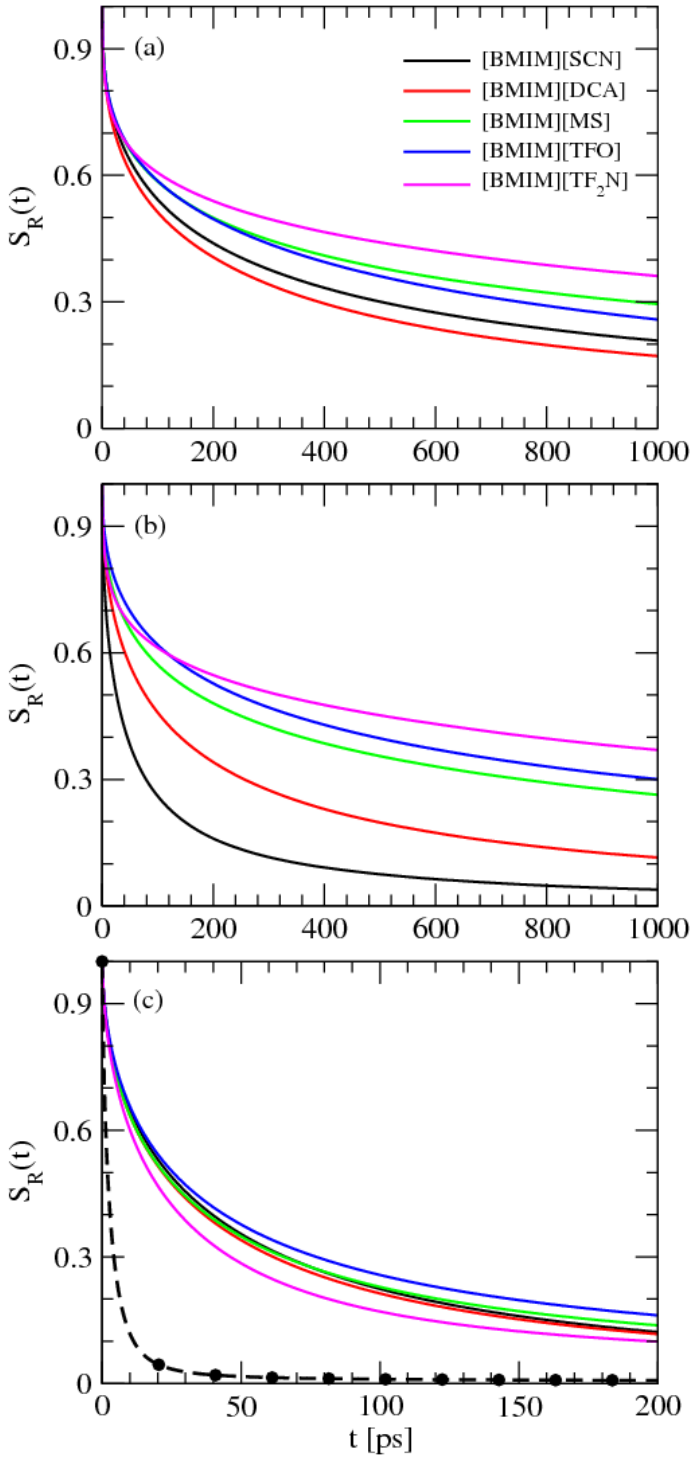

Figure 3: Relaxations of the residence time correlation function ($S_R(t)$) for (a) $BMIM^+$ cations; (b) different anions (A^-) and (c) water molecules present at the protein interface (within 6 Å) in different systems.

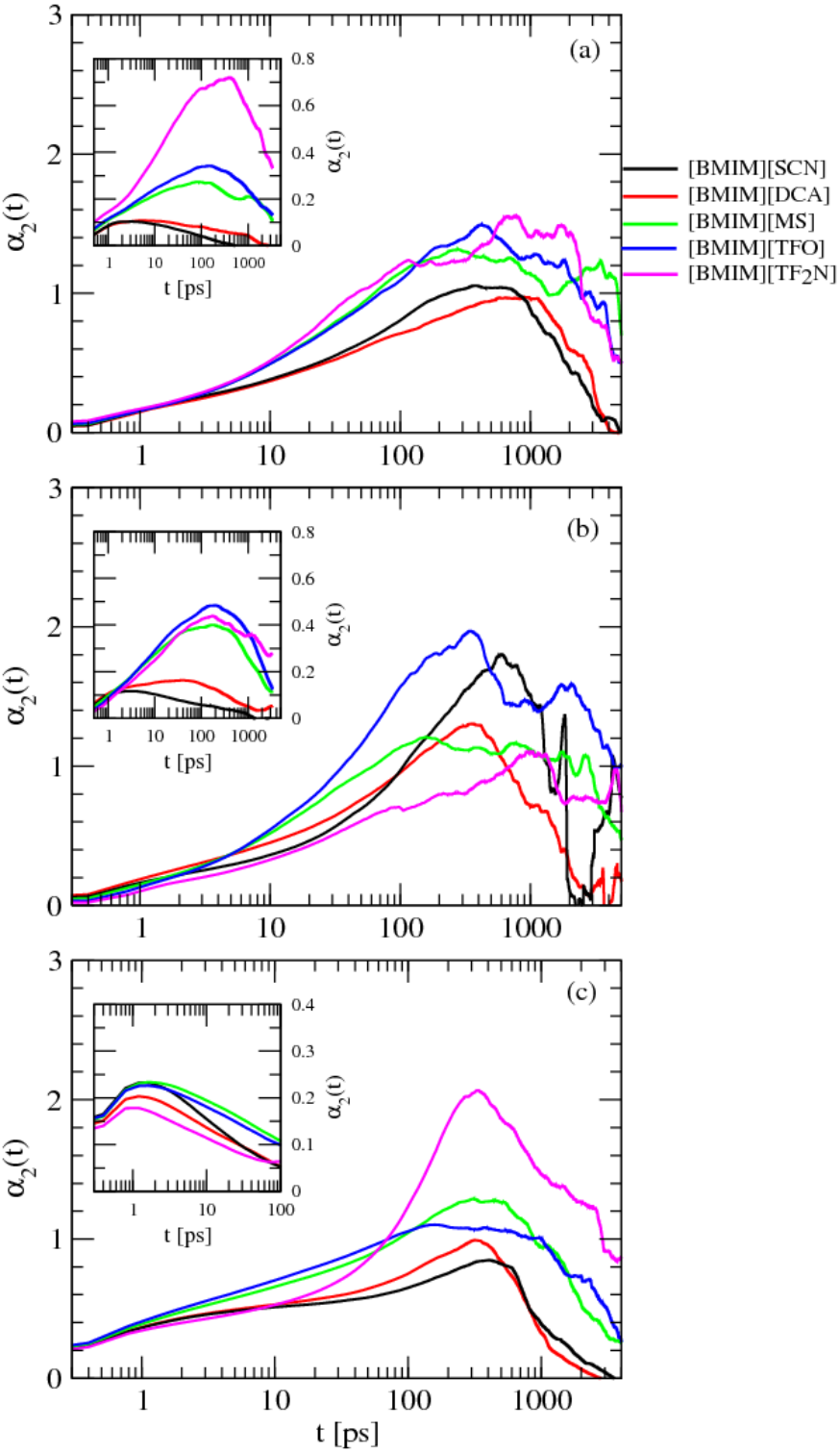

Figure 4: Time evolutions of the dynamic heterogeneity (α_2(t)) for (a) $BMIM^+$ cations; (b) different anions (A^-) and (c) water molecules present at the protein interface (within 6 Å) in different systems. The corresponding data for the bulk aqueous IL solutions in absence of the protein are shown as insets.

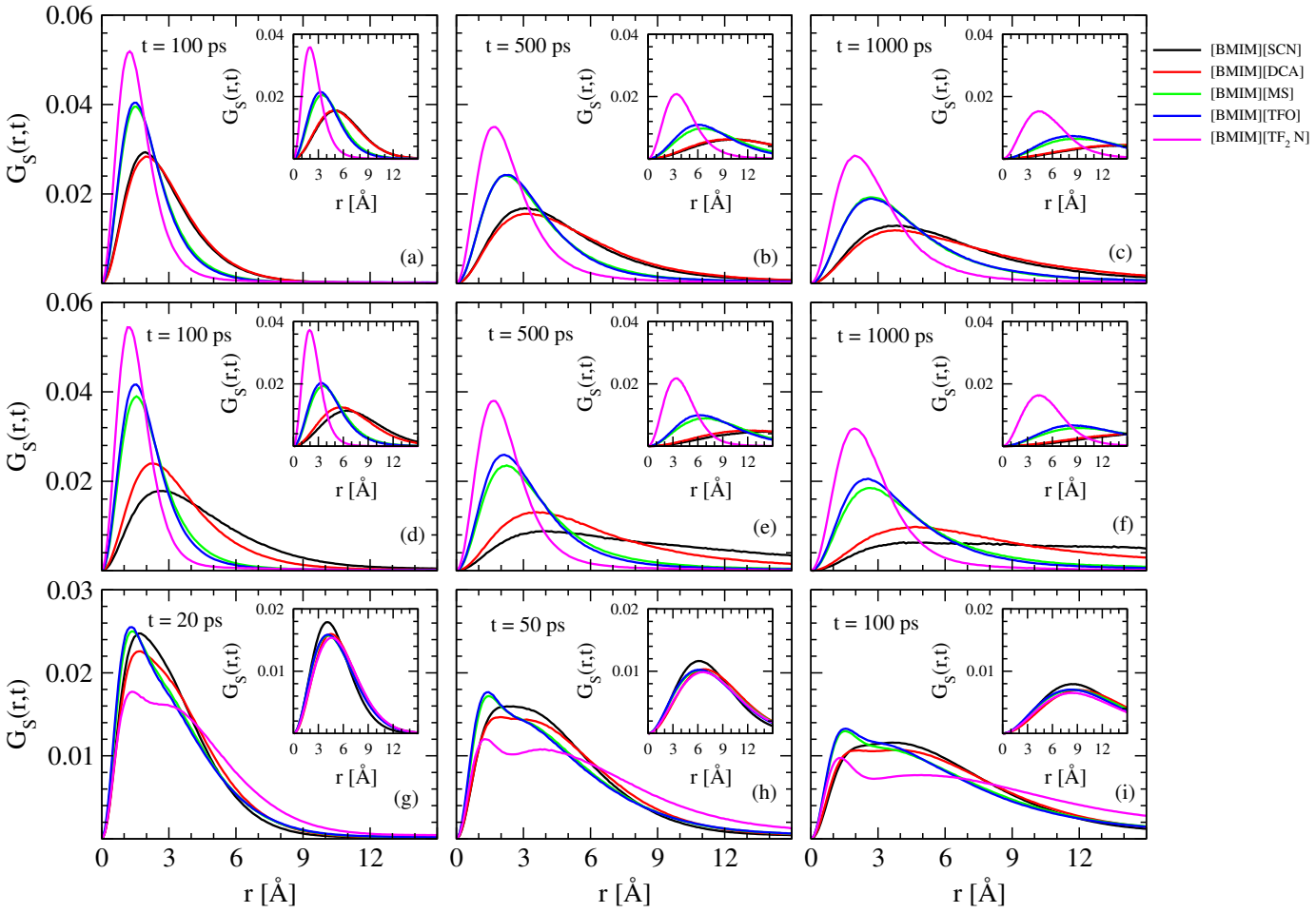

Figure 5: Time evolutions of the self-part of the van Hove correlation function ($G_S(r,t)$) for (a-c) $BMIM^+$ cations; (d-f) different anions (A^-) and (g-i) water molecules that were initially present at the protein interface (within 6 Å) in different systems. The corresponding data for the bulk aqueous IL solutions in absence of the protein are shown as insets.

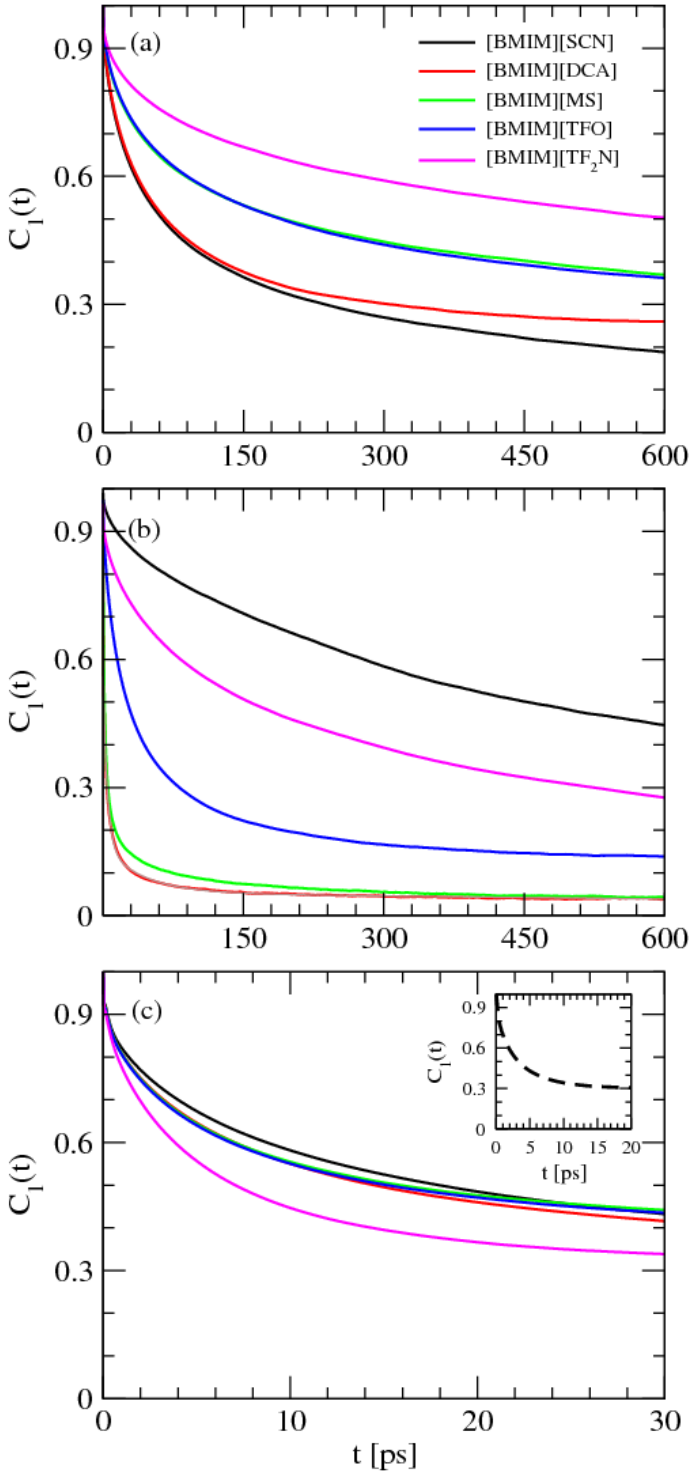

Figure 6: Relaxations of the reorientational time correlation function ($C_1(t)$) for (a) $BMIM^+$ cations; (b) different anions (A^-) and (c) water molecules present at the protein interface (within 6 Å) in different systems. The corresponding data for water around the protein in pure aqueous medium in absence of any IL is shown as inset in (c).

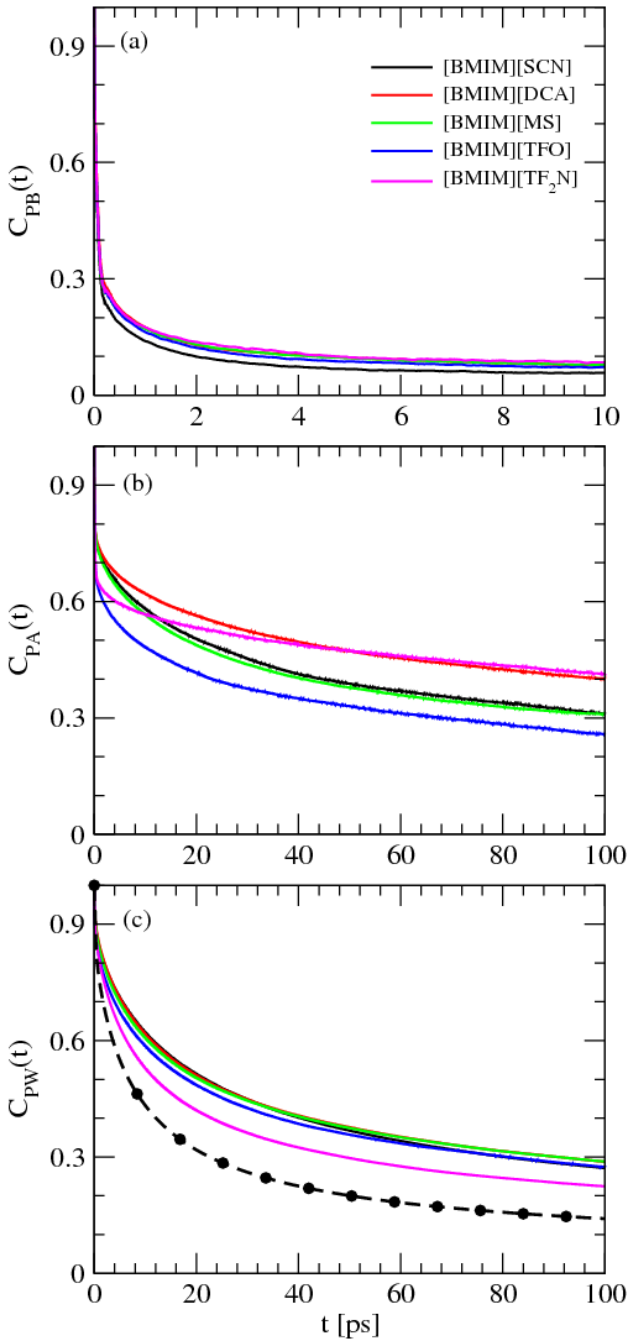

Figure 7: Relaxations of the intermittent hydrogen bond time correlation functions ($C_{PB}(t)$, $C_{PA}(t)$ and $C_{PW}(t)$) for the PB, PA and PW hydrogen bonds formed at the protein interface in different systems.

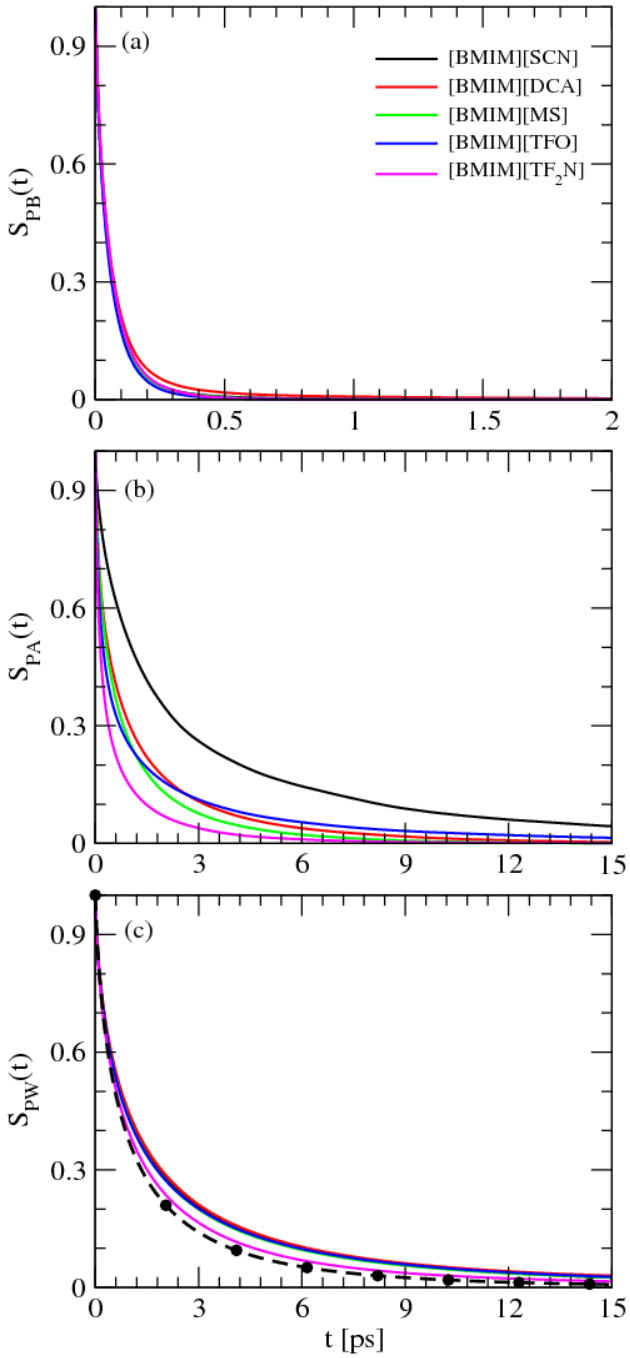

Figure 8: Relaxations of the continuous hydrogen bond time correlation functions ($S_{PB}(t)$, $S_{PA}(t)$ and $S_{PW}(t)$) for the PB, PA and PW hydrogen bonds formed at the protein interface in different systems.

“TOC Graphic”